LOCAL CALIBRATION OF MEPDG FOR SUPERPAVE PAVEMENTS IN ONTARIO: ENHANCE RUTTING CALIBRATION AND PRELIMINARY STUDY ON IRI MODEL

by

Maryam Amir

BEng, Tehran University, Iran ,2003

A thesis

presented to Ryerson University

in partial fulfillment of the

requirements for the degree of

Master of Applied Science

in the Program of

Civil Engineering

Toronto, Ontario, Canada, 2017

AUTHOR'S DECLARATION

I hereby declare that I am the sole author of this thesis. This is a true copy of the thesis, including any required final revisions, as accepted by my examiners.

I authorize Ryerson University to lend this thesis to other institutions or individuals for the purpose of scholarly research.

I further authorize Ryerson University to reproduce this thesis by photocopying or by other means, in total or in part, at the request of other institutions or individuals for the purpose of scholarly research.

I understand that my thesis may be electronically available to the public.

PAVEMENTS LOCAL CALIBRATION OF MEPDG FOR SUPERPAVE PAVEMENTS IN ONTARIO: ENHANCE RUTTING CALIBRATION AND PRELIMINARY STUDY ON IRI MODEL

by

Maryam Amir

Master of Applied Science, 2017

Civil Engineering, Ryerson University

Toronto, Canada

ABSTRACT

The AASHTO Mechanistic-Empirical Pavement Design Guide requires local calibration to account for local conditions, materials, and engineering practices. Previous local calibration studies in Ontario focused mainly on permanent deformation models for pavement rutting. The objectives of this study are twofold. First, to provide an enhanced calibration for the rutting models by using more vigilantly cross-verified input data and updated observed rutting data. Second, to perform a trial calibration for the international roughness index (IRI) model by considering three different calibration methods. Cracking models calibration, being performed by another colleague, has not yet been finalized; therefore, the IRI model calibration cannot be finalized in this study. Based upon 63 Superpave sections, the local calibration coefficients were found to be $\beta_{AC} = 1.7692, \beta_T = 1.0, \beta_N = 0.6262, \beta_{GB} = 0.0968$ and $\beta_{SG} = 0.2787$, which reduced the standard deviation of residuals to a value of 1 mm. The IRI calibration study found that the initial IRI value plays an important role in the calibration.

Keywords: International Roughness Index (IRI) model; local calibration; Mechanistic-Empirical Pavement Design Guide (MEPDG); rutting model; Superpave.

ACKNOWLEDGEMENTS

First, I would like to profess my deepest gratitude to my supervisor, Dr. Arnold Yuan. His remarkable support, suggestions, astute criticism and continuous guidance during all phases of this dissertation made this thesis possible.

I gratefully acknowledged that this research is part of a project funded by the Ministry of Transportation of Ontario (MTO) Highway Infrastructure Innovation Funding Program. My sincere thanks also goes to Mr. Warren Lee, Mr. Stephen Lee and Mr. Li Ningyuan from the MTO, Pavement and Foundation Section, for their generous and valuable help.

Also, I would like to thank all the participants of the Ryerson Research Group led by Dr. Yuan on the MEPDG Local Calibration; in particular, I would like to acknowledge and express my sincere thanks for the great help from Mr. Gyan Gautam and Ms. Chowdhury Ahmed in the early stage of my study.

Furthermore, I would like to extend my gratitude to Dr. Medhat Shehata and Dr. Bhagwant Persaud, members of the oral examination committee, for their valuable comments and suggestions along with their support and continuous guidance during my MASc study period at Ryerson.

I would also like to extend my deepest thanks to Mr. Desmond Rogan, the network administrator of the Department of Civil Engineering, for his support in network connections.

My greatest gratitude and appreciation would be towards my beloved family, whose support and love helped me throughout the entire process. I will be grateful forever for your love. Especially my mother, father and dearest sisters; there are not enough words to describe how grateful I am to all of you.

TABLE OF CONTENTS

LIST OF FIGURES

LIST OF TABLES

LIST OF APPENDICES

LIST OF ABBREVIATIONS

AADTT	Annual Average Daily Truck Traffic
AASHO	American Association of State Highway Officials, the predecessor of AASHTO
AASHTO	American Association of State Highway and Transportation Officials
AC	Asphalt Concrete
ADOT	Arizona Department of Transportation
GB	Granular Base
SG	Sub Grade
ARAN	Automatic Road Analyzer
CBR	California Bearing Ratio
ESAL	Equivalent Single-Axle Load
FHWA	Federal Highway Administration
GB	Granular base
GWT	Ground Water Table
HMA	Hot Mix Asphalt
IRI	International Roughness Index
LTPP	Long Term Pavement Performance
MEPDG	Mechanistic-Empirical Pavement Design Guide
MTO	Ministry of Transportation of Ontario
MoDOT	Missouri Department of Transportation
NCHRP	National Cooperative Highway Research Program
PMS	Pavement Management Systems
PR	Public Roads
RSS	Residual Sum of Square
SMA	Stone Matrix Asphalt

CHAPTER 1 INTRODUCTION

1.1. Background

Many studies have been performed to develop an enhanced method for highway pavement structural design. Between 1940 and 1960, under the leadership of Highway Research Board, a number of large-scale road tests were performed; the Maryland Road Test, the WASHO Road Test, and the AASHO Road Test (Yoder and Witczak, 1975). Among these, the AASHO Road Test is the most important. It was the first road test to quantify an empirical connection between pavement performances and influencing factors such as structural design and varying axle loads. The empirical equations were adopted in the first Interim Guide for Design of Rigid and Flexible Pavements, published in 1961. With modifications based upon subsequent studies, these equations continued to be used until the 1993 AASHTO design guide.

The major disadvantage of the empirical method is the limited range of parameters in terms of structural design, materials, traffic loading, environmental and climatic conditions, and maintenance practices that the original AASHO Road Test could support. As axle loads increase, new materials are developed, and climate changes, the empirical equations have been found to be inappropriate and their performance predictions unjustified. At the dawn of the twenty-first century, progressive pavement engineers decided to overthrow the empirical design method and develop a new method that had more mechanistic underpinnings. This ambition resulted in the Mechanistic-Empirical Pavement Design Guide (MEPDG), the product of a joint effort by AASHTO and FHWA under the NCHRP project 1-37A.

The MEPDG was developed to find the cause and effect of stresses in pavement performance indices. Within MEPDG, we initially assumed a trial design, along with inputs for traffic and climate conditions. Using this information, mechanistic models calculate pavement responses (stress strain, deflection), Pavement responses are converted to distress predictions (Rutting, Cracking and IRI) by empirical models in the software.

In project 1-37A, the empirical models were calibrated using the Long-Term Pavement Performance (LTPP) database. Since the database used in the calibration covers pavement design from a large portion of the USA and some provinces in Canada, including Ontario, the calibration is called global calibration. However, from the outset of MEPDG development it has

been expected that globally calibrated models may inaccurately predict pavement performance in response to some local conditions. Hence, for those user agencies, software output cannot be a precise representation of current or future pavement performance.

The MTO decided to allocate budget from Highway Infrastructure Innovation Funding for further research on this topic. For Ontario's flexible pavements, Ryerson research group concluded that the MEPDG should be locally calibrated for its rutting, cracking and IRI models.

1.2. Motivation and Significance

The goal of calibration, either global or local calibration, is to produce the most accurate (non-bias) and precise (reliable) prediction of pavement performances (figure 1).

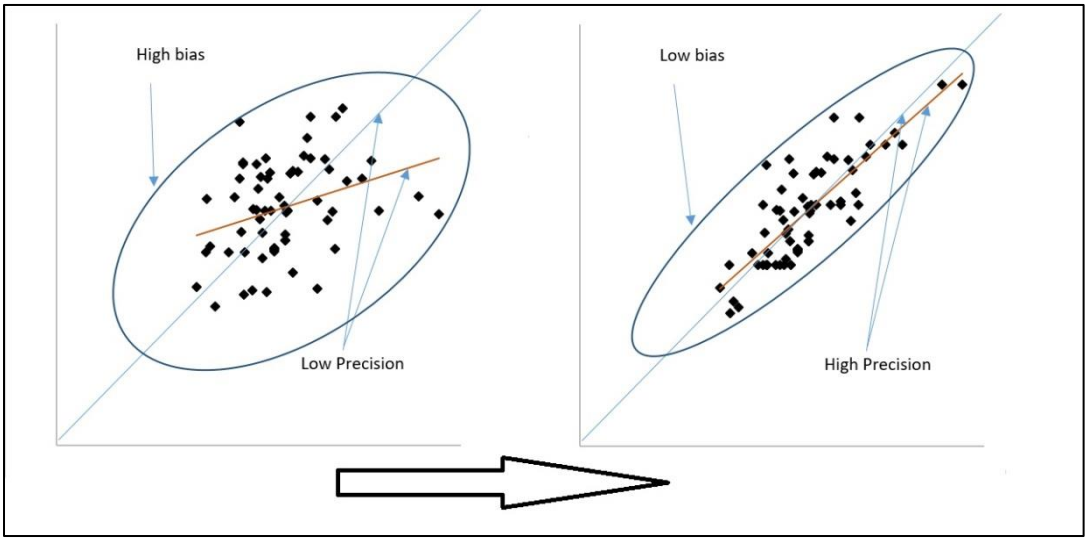

Figure 1. Precision and bias in local calibration

The MTO, as a leading transportation agency, is mandated to adopt the AASHTO MEPDG. For future design, preliminary studies within the MTO showed that transfer models needed to be calibrated. Since 2010, a Ryerson research group led by Dr. Yuan has been tasked to conduct the local calibration. The study started with the development of a local calibration database. In this project, Jannat (2012) developed a database that later turned out to predominantly cover the Marshall type of mixes, which are no longer used by the MTO. Nevertheless, using this database, Jannat (2012) confirmed the dire need for local calibration of the rutting models and identified the major challenges that would be faced if the cracking models were to be calibrated. She further confirmed the need for calibration of the IRI model, although the extent of bias and residuals in this model was less than that found in the other distress

models. Based upon her study, the research group, upon discussion with the MTO, established local calibration priority in the following order: rutting models first, followed by cracking models (fatigue, thermal), and concluding with IRI.

Using the same calibration database, Waseem (2013) performed a sophisticated rutting model calibration, in which he identified the major challenge of rutting model calibration to be the unknown layer contributions among asphalt concrete (AC), granular base and subbase, and subgrade soil. Using the observed rutting series from PMS database, Waseem also experimented with a section-by-section longitudinal calibration method, which was the first attempt at a local calibration study in North America. He also developed a semi-automated calibration procedure, which could drastically improve the efficiency of the calibration exercise.

Later on, the study group realized the defect in the local calibration database. Therefore, for subsequent studies, the group developed a new calibration database for Superpave, which has been used in Ontario since 2001. Based upon the new database, Gautam (2015) recalibrated the rutting model and compared the results of Marshall mixes and Superpave materials. In addition, he made a great effort to enhance the local calibration method by identifying the local calibration coefficients that should be set using prior information and the coefficients that could be identified through the regression analysis.

Gautam (2015) suggested that the traffic and temperature exponents in the AC rutting model could be set at a specific value based on the most recent rutting study, NCHRP project 9-30A. In doing so, the indeterminacy issue due to lack of layer contribution was largely reduced, if not completely resolved. However, the data in his study resulted in zero or close-to-zero coefficients in the subgrade or base/subbase models, which was a major drawback of the calibration result. This was the motivation the first part of this study; Amir (2017), to further enhance the local calibration of rutting models.

Regarding IRI model calibration, as mentioned before, this was intended to be the last transfer model to be calibrated. Within the research group, Ahmed (2017) conducted a parallel study, focusing on the cracking models. Unfortunately, cracking model calibration was not successfully completed before this study started. As a result, it was decided that IRI calibration in this study would focus on exploration of the best calibration method. Therefore, this work represents a preliminary study using uncalibrated cracking models.

1.3. Objectives

The objectives of this study are: firstly, to perform an enhanced calibration for rutting models by revising the input database; and secondly, to perform a trial calibration of the IRI model using three different calibration methods. To accomplish these tasks, coefficient values of the models will be revised in such a way that the most accurate (non-biased) and precise (reliable) predictions of observed values can be obtained. The local calibration database will be developed based on typical Ontario's Superpave and SMA pavement sections under MTO's jurisdiction.

1.4. Research Methodology

Based on the literature review performed for this study, it was apparent there was an immediate need to enhance current calibrated rutting models and to perform a preliminary local calibration on the latest global IRI model for Ontario's flexible pavement. The calibration strategy used in this research was cross sectional or, as named by Waseem (2013), a pooled calibration method. By cross-sectional calibration, author means to perform calibration on a pool of rutting measurement values. An enhanced calibration database was built upon the one previously developed and used by Jannat (2012), Waseem (2013) and Gautam (2015). For the purpose of this study, a total of 63 sections were selected and their raw observed IRI and rut depth data were extracted from Ontario's PMS 2015 database. Since the methodology of measuring rut depth and IRI has changed over the past few years, this study only uses the 2015 database for analysis.

For this study, the latest version of the MEPDG software (V2.3) was used. Using output from the software, rutting and IRI calculation procedures were simulated within an Excel file. Finally, using least square linear regression technique, local calibration was performed to produce a non-bias and precise performance prediction model.

To maintain the integrity and validity of the result, for rutting, the effects of zero bias constraint on the produced standard error was evaluated using two methods. The IRI model is a function of pavement distress over time. Because cracking model calibration had not been completed prior to this study, the predicted IRI results from the default global model were not up to date. Meanwhile, the initial IRI (IRI_0) value was found to have a governing effect on the final predicted value of IRI. Therefore, three methods based on different IRI_0 values were proposed to explore the best approach for performing local calibration of the IRI model.

1.5. Thesis Organization

The thesis is divided into five chapters and three appendices. This first chapter presents the background, motivation, objectives and methodology of the study as well as thesis organization. Chapter 2 summarizes the result from a literature review on rutting and IRI models with a focus on global and local calibration studies. Chapter 3 is dedicated to the enhanced rutting calibration and highlights major differences between the current research results and previous studies. Chapter 4 is devoted to the preliminary IRI model calibration, with an emphasis on the discussion of the best methods to be used for a successful local calibration of the IRI model. Chapter 5 concludes the thesis with a summary, conclusions and recommendations for future study. The three appendices provide more detailed information, including material properties and structural information, in addition to summarized information on climate, traffic and other input data to be used in AASHTOWare Pavement ME design.

CHAPTER 2 LITERATURE REVIEW

2.1. Rutting and the Rutting Models

Rutting is one of the pavement distresses that may occur in flexible pavement due to repeated traffic load, plastic shear deformation and material densification. To measure rut depth, an automated road analyzer (ARAN) system has been used by the MTO since the late 1990s. The first-generation ARAN contained ultrasonic sensors spaced at 4-inch intervals along the bar in order to cover the full width of a lane and to produce a cross-sectional profile of the pavement surface. Figure 2 represents the second-generation system, or the ARAN-9000 vehicle, which uses a laser rut-measurement system (LRMS). This system provides a higher resolution of 1280 points per profile. The new system has an expected measurement precision of ±1 mm.

Figure 2. Laser rut measurement system (MTO 2016)

The most important part of project 1-37A was a calibration of distress transfer functions in order to adopt the design with the industry (NCHRP 719). The process of using calculated pavement responses data from MPEDG through the transfer function to predict what we actually measured in pavement surface (observed data) is calibration, which is not only model fitting but also confirms the data quality.

To provide an unbiased model for pavement distress and a reasonable standard error for pavement performance prediction, a validation of global calibration has been successfully performed for MEPDG under NCHRP project 1-37A. Data gathered for this project was from 136 sections using varied type of soil, climate, traffic and structural data. A total of 94 LTPP sections were used for calibration and validation of new construction pavements. Data from 42

LTPP sections were used for calibration and validation of AC-over-AC overlay. Sections with the following materials were excluded:

- PMA (polymer-modified asphalt)
- RAP (recycled asphalt pavement)
- WMA (warm-mix asphalt)

Under project 9-30A, the original rut-depth model (Kaloush) was enhanced in addition to adding and calibrating following rut-depth transfer function models:

- Verstraeten deviator stress-based transfer function
- WesTrack shear strain, shear stress transfer function
- Improved versions of MEPDG software (Leahy, etc.)

Model evaluation in NCHRP project 9-30A was based on their accuracy, sensitivity to HMA mixture volumetric properties such as aggregate blend and its sensitivity to temperature and robustness (Von Quintus et al., 2012).

For the new version of MEPDG, AASHTO decided to include just the original rut depth transfer functions. The following presents a summary of the latest rutting models for the AC and unbounded materials:

2.1.1. MEPDG AC Rutting Transfer Function

$$\varepsilon_{p(HMA)} = \varepsilon_r K_z \beta_{AC} 10^{k_{r1}} (T)^{k_{r2}\beta_T} (N)^{k_{r2}\beta_N} \quad (1)$$

where

ε_r =Resilient strain (HMA layer), mm/mm

ε_p =Accumulated plastic strain (HMA layers), mm/mm

T =Pavement or mix temperature, ^{0}C

N =Number of load application of a particular axle type

$\beta_{AC}, \beta_N, \beta_T$ =local calibration coefficients

K_{r1} =Plastic deformation factor, for global calibration equals to -3.35412

K_{r2} =Plastic deformation factor based on temperature effect, for global calibration equals to 1.5606

K_{r3} = Plastic deformation factor based on wheel loads effect, for global calibration equals to 0.4791

K_Z =Depth function, $K_Z = (C_1 + C_2 D)(0.328196^D)$

C_1 $=-0.1039H_{HMA}^2 + 2.4868H_{HMA} - 17.342$

C_2 $=0.0172H_{HMA}^2 - 1.7331H_{HMA} + 27.428$

D = Mid depth of related layer, mm

H_{HMA} = Thickness of HMA layers, mm

2.1.2. Base/ Subgrade Rutting Transfer Function

$$\left(\frac{\varepsilon_P}{\varepsilon_v}\right) = \beta_{GB-SG}\, k_{s1} \left(\frac{\varepsilon_0}{\varepsilon_r}\right) e^{-\left(\frac{\rho}{n}\right)^{\beta}} \quad (2)$$

ε_p = Accumulated plastic strain (Base/ Subgrade layers), mm/mm

N = Number of load application of a particular axle type

ε_0 = Material properties gained from repeated load permanent deformation test in laboratory, mm/mm

ε_r = Resilient strain value from laboratory test which help to obtain ε_0, ρ and β, mm/mm

ε_v = Average vertical elastic strain obtained from structural response model, mm/mm

k_{s1} = Global calibration coefficients; if fine grained material, value would be 1.35 and for granular material would be 2.03

β_{GB-SG} = local calibration coefficients, for global calibration equal to 1.0 for both fine grained and granular materials

$log\beta$ $=-0.61119 - 0.017638(W_c)$

W_c = Water content, %

ρ $=10^9 \left(\left(\frac{C_0}{1-(10^9)^{\beta}}\right)\right)^{1/\beta}$

C_0 $= ln(\frac{a_1 M_r^{b_1}}{a_9 M_r^{b_9}})$=*-4.89285*

M_r = Resilient modulus of the unbound layer or sublayer, psi

$a_{1,9}$ = Regression constants; a_1=0.15 and a_9=20.0

$b_{1,9}$ = Regression constants equals to zero

As mentioned before, the global models overestimate the total rut depth for Ontario roads. In the following, the results of previous local calibration studies for Ontario's roads performed by the Ryerson research group team on rutting models are reviewed.

For the first attempt in Ontario to calibrate rutting models for flexible pavements, Jannat (2012) developed a database. Using ME version 2 with this Marshal Mix flexible pavements database, the Jannat, Yuan and Shehata (2014) analysis showed overestimated rutting values for Ontario's flexible pavement sections. To develop a more precise regression equation for local calibration of rutting, they recommended clustering the database based on highway classes. As mentioned before, the main goal of local calibration is to eliminate bias and to reduce the RSS. For RSS minimization, it is commonly expected that by using the appropriate optimization toolbox, unique optima would be generated. A study performed by Waseem and Yuan (2013) showed multiple local optima within the optimization process. Based on their study, unknown layer contribution to rutting was the main cause of the phenomenon of multiple local optima. To address the issue of layer contribution to the rutting model, Waseem (2013) attempted a sophisticated local calibration of the rutting model for Ontario's Marshal Mix flexible pavements. Waseem decided to use a 50% layer contribution for both AC and granular layer individually and to set a zero contribution for the subgrade layer in the case of rehabilitated pavements. For new or reconstructed studies, following the layer contribution measured by AAHTO in 1962, he decided to use 32% for AC, 59% for granular layers and 9% for subgrade layers. In the Waseem and Yuan (2013) study, the authors proposed a new approach of longitudinal (section-by-section) calibration for performing a local calibration study. That resulted in the following range of coefficient values: AC layer coefficient values: β_{AC}= 0.14 to 0.47, β_N=0.975 to 1.738 (effect of temperature on permanent deformation) and β_T=0.229 to 1.105 (effect of traffic on permanent deformation).

In addition, Waseem (2013) decided to perform a cross-sectional local calibration study, which resulted in the following local calibration coefficients: β_{AC}= 0.19, β_N=1.23, β_T=0.77, β_{GB}=0.985 with prefix value of β_{SG}=zero. His coefficient resulted in an improved R^2 value of 0.464 and reduced standard error equal to 1.608 mm comparing to global values.

Waseem (2013) analysis was based on the Marshal Mix flexible pavements database. From 2001, the MTO began to use Superpave material rather than Marshal Mix, which demonstrated an immediate need for the inclusion of Superpave sections in calibration studies.

Therefore, Gautam (2015) performed a local calibration study on rutting models for both Marshal Mix and Superpave pavement sections to investigate the need of different set of coefficients for the mentioned pavement types.

To simplify his analysis, Gautam (2015) decided to use prefixed values for both traffic and the temperature exponent. Based on equation 1, temperature (n) and traffic coefficient (m) refer to the exponent part of temperature and number of load application indices (n=$K_{r2}\beta_N$, m=$k_{r3}\beta_T$). To find the best prefixed values, he performed an analysis on results derived from NCHRP project 9-30A and NCHRP report 719.

Within NCHRP project 9-30A, a total of 60 field section were used to perform trench investigation and 46 laboratory samples were used to perform shear and repeated load triaxle tests. Within NCHRP project 9-30A, using rutting results derived from the mentioned tests, longitudinal calibration was performed to determine the temperature and traffic coefficients of the rutting model. Based on result derived from NCHRP project 9-30A, Gautam performed statistical and sensitivity analyses to introduce an appropriate value for a local calibration study for Ontario's flexible pavements. His analysis resulted in a traffic exponent of $n = K_{r2}\beta_n$ equal to 0.3 and temperature exponent $m = k_{r3}\beta_T$ equal to 1.5606. In equation 1, the value of global filed calibration parameters (k_{r2} ,k_{r3}) is equal to 0.4791 and 1.5606. This resulted in prefixed values of 0.6262 and 1 for β_N and β_T respectively. This study used the same values for its AC rutting model local calibration.

Since the focus of the current study is on Superpave sections, Gautam (2015) calibration result for Marshal Mix sections will not be included. Similar to Waseem (2013), he used both longitudinal and cross-sectional approaches to perform local calibration of rutting models. his cross-sectional calibration resulted in the following coefficient values: β_{AC}= 2.692, β_{GB}= 0.000 and β_{SG}= 0.185 with average layer contribution of 31.21%, 0.00% and 68.79%.

Gautam (2015) results, was succeeded to reduce the standard error value to 1.2 mm, yet having a zero contribution of the granular layer to rutting was far beyond reality. For further details of Ryerson work's in previous rutting model calibration, refer to Gautam et al. (2016).

Local calibration studies on both rutting and IRI models have been performed by many regional agencies through North America. A comprehensive literature review on rutting models has been performed by Gautam (2015). Section 2.3 of this study is mainly focused on a literature review for IRI models.

2.2. Pavement Smoothness and the IRI Model

IRI, one of the pavement performance indicators, stands for international roughness index. It measures the surface roughness for any pavement type. The MTO uses ARAN to measure IRI and other pavement performance indicators for Ontario's highway. In January 2010, the existing ARAN vehicle was replaced by the latest version of ARAN. The new version contains almost all of the previous subsystems, such as GPS, Laser SDP, etc., as well as some further improvements. The new ARAN vehicle consists of the following instruments:

- Three sets of cameras, to collect images every 20 feet as ARAN travels along the highway.
- High-speed laser distance measurement system, utilizing 36 ultrasonic sensors to measure rutting and roughness along the road.
- High-speed laser distance measuring system, consist of two infrared lasers and accelerometers along the wheel path to measure roughness along the road.
- GPS to detect and store the location of each datum.
- DMI (distance measuring instrument).
- Three onboard computers.

To calculate IRI, longitudinal profile data for the road are captured continuously using both laser and accelerometer instruments (RoLine Laser inertial profiler). Sample of roughness profile generated by ARAN can be found in figure 3.

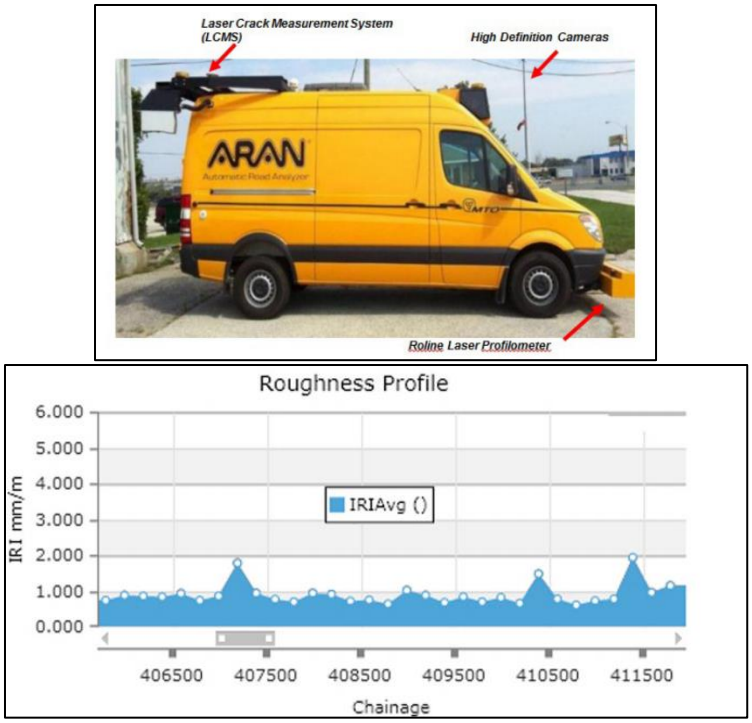

Figure 3. MTO ARAN 9000 longitudinal profile data (MTO 2016)

In the AASHO Road Test, roughness was presented as present serviceability rating (PSR) which was scaled from zero (very poor) to five (excellent). Value was determined based on traveller interpretation of their ride comfort. Later on, an effort was made by AASHTO to find an actual correlation between ride comfort and pavement distresses, which led to major findings on the correlation between smoothness of the road, its rut-depth variation and the severity of cracks.

Based on the study performed by the Transportation Research Board of Washington, DC, a relationship is observed between the smoothness of a road and its design structure, climate and site conditions.

The first empirical IRI model was developed by Darter and Al-Omari (1992), representing a significant relationship between IRI and variation of rutting along the road. Within same study, significant correlation was observed between number of transverse cracks, potholes, swells, depressions and the smoothness of the road.

In NCHRP project 1-37A, an enhanced IRI model was evolved to introduce the relationship between road smoothness and pavement distresses. To develop an IRI model for flexible pavements, distress data was gathered from an LTPP database for different types of flexible pavements. Based on new and overlaid flexible pavements, data was separated into two separate groups. In addition to the data cleaning process, one major task was to develop an

appropriate estimation of initial IRI values for each section. Considering the direct relationship between IRI trend and pavement age, a back calculation method was used to fit a linear model for the trend of IRI versus their pavement age within the service life of each section. Stepwise regression was performed on 493 new and 61 flexible overlaid pavement data points, which led to two separate models for new and overlaid flexible pavement.

Another important variable influencing the rate of pavement smoothness deterioration,was found to be flexible pavement base type, such as granular, asphalt-treated and cement-treated base. Therefore, the IRI model was modified based on pavement base type cluster regression.

The following represents the current MEPDG IRI model for flexible pavement with granular base:

2.2.1. MEPDG International Roughness Index Transfer Function

$$IRI = IRI_0 + C_1(RD) + C_2(FC_{Total}) + C_3(TC) + C_4(SF) \quad (3)$$

IRI = Predicted IRI, in/mi

IRI_0 = Initial IRI after construction, in/mi

FC_{Total} = Area of fatigue cracking (combined alligator, longitudinal, and reflection cracking in the wheel path), percent of total lane area

TC = Length of transverse cracking, feet/mile

SF = Site factor

RD = Average rut depth, inches

C_1, C_2, C_3, C_4 =IRI model calibration factor, equal to 40, 0.4, 0.008, 0.015 respectively

$$SF = (Frost) + Swell(Age)^{1.5} \quad (4)$$

Frost $=\{\ln[(P_{recip} + 1)(FI + 1)p_{02}]\}$

Swell $=\ln[(P_{recip} + 1)(PI + 1)p_{200}]\}$

P_{recip} =Mean annual precipitation(mm)

FI = Mean annual freezing index (ºC – days)

$P_{0.02}, P_{200}$ =Percent of subgrade material passing 0.02mm and 0.075μm sieve respectively

Following is current IRI standard deviation model for flexible pavements based on Alex Gotlif ARA/TRANS, e-mail message to author, November 4, 2016. IRI standard deviation model is hardcoded in the software therefore users cannot change them.

$$S_{e(IRI)}^2 = Var_{IRI_0} + C_2^2 Var_{bot} + C_3^2 Var_{Thermal} + C_1^2 Var_{Rut} - Var_{IRIMeas} - C_1^2 Cov_{Rut}^2 Rut_{Tot} - C_2^2 Cov_{Bot}^2 Crack_{Tot} - C_3^2 Cov_{Tran}^2 Crack_{Trans} + S_e^2 \quad (5)$$

where:

$S_{e(IRI)}^2$ = Standard deviation of IRI at the predicted level of mean IRI

Var_{IRI_0} = Variance of initial IRI (obtained from LTPP) = $(IRI_{ini}/10)^2$, $(in/mi)^2$

Var_{bot} = Variance of bottom-up cracking, $(percent\ lane\ area)^2$

$Var_{Thermal}$ = Variance of thermal cracking, $(ft./mile)^2$

Var_{Rut} = Variance of total rutting (all rutting sub-models), $(in)^2$

$Var_{IRIMeas}$ =Variance of initial IRI measurement=0.4472, $(in/mi)^2$

Cov_{Rut} =Coefficient of variation of the rutting measurement=0.2

Rut_{Tot} =Total rutting, (in)

Cov_{Bot} =Coefficient of variation of the bottom cracking measurement=0.38

$Crack_{Tot}$ =Total fatigue cracking, (percent of lane area)

Cov_{Tran} =Coefficient of variation of the bottom cracking measurement=0.09

$Crack_{Trans}$ =Total transverse cracking length (ft. /mile)

S_e^2 = Variance of overall model error, $(in/mi)^2$

S_e^2 =25.1148LN (IRI)-87.95062

Jannat (2012) developed a local calibration database featuring Marshall-type mixes. Using this database, she performed a study to validate the IRI global model for Ontario conditions. To produce an optimized predicted model for IRI, Jannat suggested to cluster IRI database based on Ontario's zones. Marshall-type mixes are no longer used by the MTO, so her database could not be used for this part of the study. As mentioned before, during sequence planning for MEPDG local calibration for Ontario, it was decided that calibration of IRI model

would be the last step, therefore current study would introduce the first effort to perform a trial calibration for the IRI model.

2.3. Calibration Factors - Previous Local Calibration Studies

Local calibration studies on both rutting and IRI models have been performed by many regional agencies through North America. A comprehensive literature review on rutting models has been performed by Gautam (2015), so this section mainly focuses on a literature review for IRI models.

For Missouri, Donahue (2008) performed a local calibration of the IRI model after calibrating rutting and transverse cracking models using MoDOT and LTPP databases. The bias after calibration seemed to be acceptable, although not all the null hypothesis tests resulted in p-values more that 5 %. Compared to global validation results, the local calibration effort generated better results with a reduced S_e value equals to 12.8 inch/mile.

For Iowa, Gopalakrishnan et al. (2013) performed a study on local calibration for Iowa flexible pavements. Longitudinal cracking and thermal cracking model calibrations were still evolving and the accuracy of the national calibrated IRI model seemed to be acceptable for Iowa conditions, having bias of 0.67 inch/mile with S_e value equal to 12.35 inch/mile. Therefore, it was decided to use global IRI model.

For Arizona, using the global calibration coefficient for predicting the IRI value resulted in imprecise prediction. Local calibration for the IRI model was performed by Darter et al. (2014) using 180 pavement sections from the LTPP and ADOT pavement management database, which led to reasonable prediction of IRI with reduced standard error equal to 8 inch/mile.

For Colorado, Mallela et al. (2013) performed a validation study on the MEPDG IRI global model for Colorado's flexible pavement, which indicated imprecise prediction of IRI. Therefore, an effort was made to perform a local calibration of the model for Colorado's flexible pavement by using 343 sections. This led to significant improvement in elimination of bias with reduced standard error equal to 17.2 inch/mile.

For Ohio, using the global calibration coefficient for predicting the IRI value resulted in biased prediction. In order to eliminate bias, Glover and Mallela (2009) performed a local calibration of the IRI model for Ohio's local conditions. After local calibration, a decent correlation between observed and predicted IRI was observed. Although bias was not eliminated

entirely, local calibration results seemed to be more acceptable than global ones and resulted in a reduced standard error equal to 15.9 inch/mile

Table 1. Calibration factors from previous studies - IRI model

State	Factors	Local	References
Missouri	$C_1(RD)$	17.7	Donahue (2008)
	$C_2(FC_{Total})$	0.975	
	$C_3(TC)$	0.008	
	$C_4(SF)$	0.01	
Iowa	$C_1(RD)$	40	Gopalakrishnan et al. (2013)
	$C_2(FC_{Total})$	0.4	
	$C_3(TC)$	0.008	
	$C_4(SF)$	0.015	
Arizona	$C_1(RD)$	1.2281	Darter et al. (2014)
	$C_2(FC_{Total})$	0.1175	
	$C_3(TC)$	0.008	
	$C_4(SF)$	0.028	
Colorado	$C_1(RD)$	35	Mallela et al. (2013)
	$C_2(FC_{Total})$	0.3	
	$C_3(TC)$	0.02	
	$C_4(SF)$	0.019	
Ohio	$C_1(RD)$	17.6	Glover and Mallela (2009)
	$C_2(FC_{Total})$	1.37	
	$C_3(TC)$	0.01	
	$C_4(SF)$	0.066	

CHAPTER 3 RUTTING MODEL CALIBRATION

3.1. Introduction

As mentioned before, the main focus of this study will be on recalibrating the rutting models for Ontario's Superpave pavements. General frame work would be performing calibration on the pool of rut depth measurement values which was named Cross sectional calibration by Ryerson research group team. Database includes only 2015 database; one-year selection was based on the fact that measurement methodology in ARAN continues to change in the last few years. To perform local calibration split sample method was used. For calibration purpose software procedure was simulated within an Excel file. At the end a non-bias and precise performance prediction model was introduced using least square linear regression technique.

3.2. Local Calibration Database

3.2.1. Projects and Sections

The local calibration database used in this study was built upon previous database that were originally developed and used by Waseem (2013), Gautam (2015) and Ahmed (2017). A total of 148 Superpave sections were originally identified and processed by the previous studies. However, only 63 of the sections were found to be appropriate for the purpose of this study. Effort has been made to produce a clean accurate database. The following are the criteria considered to select those sections:

- The selected sections should be a comprehensive representative of the set of materials, geotechnical conditions and structural designs in Ontario. Therefore, the selected sections include projects from both southern and northern Ontario.
- MTO (2011) reintroduced Stone Mastic Asphalt (SMA) to the list of approved premium surface mix for its relatively high rut resistance characteristic after its surface friction issue was resolved. Therefore, unlike previous studies this study database included SMA sections as well.
- The construction type should be either a new construction or an AC-over-AC rehabilitation pavement.
- Since the MTO's PMS database does not maintain accurate construction and maintenance

records, each section was carefully assessed by using their time-series performance data to accurately determine the maintenance and rehabilitation history and thus the year of its latest major rehabilitation. Sections with service life of less than 3 years was eliminated.

- For all of the sections, raw observed data for rut depth was extracted from Ontario's PMS 2015 database. The one-year selection was based on the fact that measurement methodology in ARAN continues to change, and the data are not consistent from year to year. As mentioned in chapter 1, a previous study on rutting models was based on a PMS database up to 2012. The PMS 2015 database has been generated from the latest ARAN methodology with highest accuracy so far. Therefore, using the 2015 database will be result in a reduction of measurement variance.
- To improve the calibration result it would be better to include sections with performances outside the range of critical values stated in table 2. But unfortunately, the available observed IRI values within this study varied from 0.7 - 1.7 m/km and observed rut depth data ranged from 2.4 to 6.7 mm. This could result in less precise prediction for both models.

Table 2. Summary of rut-depth and IRI thresholds (MTO 2016)

Performance Criteria	Limit	Pavement Type	Highway type
IRI	1.9	Superpave	Freeway
	2.3		Arterial
	2.7		Collector
	3.3		Local
Rut Depth	10	Superpave	Freeway
	13		Arterial
	17		Collector
	17		Local

- New section structural information has been partially re-created from available MTO report, to make sure of the accuracy and completeness of their pavement design structure database.
- Summary of the location, material and structural information for the selected Superpave sections can be found in table A-2 and table A-2.

3.2.2. Climate Information

For each section the average of several nearest weather station was found and selected from the "Weather stations for MEPDG in Ontario", accessed January 16, 2017, https://www.google.com/maps/d/viewer?msa=0&mid=13iBJ4hBSeGc_gTw_KJsEtwHXPXk. Based on mentioned website a total of 34 weather stations is available within Ontario, database for those station would be updated by AASHTO occasionally (see figure 4).

Figure 4. Location of the 34 Ontario climate stations (MTO 2016)

Climate input information used for this study can be found in table B-1 and table C-5.

3.2.3. Pavement Structures and Materials

The focus of this study is on flexible pavements with typical structure of AC layers and unbound layers. Section selection was expanded by including SMA sections as well, and their information was revised and modified completely.

AC layer for this study includes following Superpave materials:

- Stone matrix asphalt (SMA)
- Superpave 12.5 mm (SP12.5)
- Superpave 12.5 mm friction course 1 (SP12.5 FC1)
- Superpave 12.5 mm friction course 2 (SP12.5 FC2)
- Superpave 19 mm (SP19)

- Superpave 25 mm (SP25)

Detailed specification for asphalt material can be found in table C-1. Unbound material includes typical Ontario's granular and fine materials, which has been reported in table C-2 and C-3 of this study. Used input information for AC and unbound layers can be found in table B-3.

3.2.4. Traffic Information

Section selection was based on an effort to including diverse Ontario traffic conditions in this study. For each section based on their LHRS information, traffic data was obtained from iCorridor website. However, since some AADTT information was found to be not completely precise, AADTT information of each section was compared by their available information within the MTO traffic database. Summary of traffic inputs used for this research can be found in table B-2.

3.2.5. Hierarchical Input Levels

Summary of input level used for this research can be found in table 3. Based on available information, input level 3 was used for the purpose of this study. In this level, default regional or national inputs will be used.

Table 3. Summary of input level

Input Group /Input Parameter	**Input Level Used**
Truck Traffic	
Axle Load Distributions	Level 2
Lane & Directional Truck Distribution	Level 2
Truck Volume Distribution	Level 2
Axle Configuration, Tire Spacing	Level 3
Truck Wander	Level 3
Tire Pressure	Level 3
Climate	
Wind Speed, Temperature, Cloud Cover, Precipitation, Relative Humidity	Level 2
HMA layers Material Properties	
Volumetric Properties	Level 3
HMA Creep Compliance and Indirect Tensile Strength	Level 3
HMA Dynamic Modulus	Level 3
HMA Coefficient of Thermal Expansion	Level 3
Unbound layers Material Properties	
Resilient Modulus –All Unbound Layers	Level 3
Moisture-Density Relationships	Level 3
Classification and volumetric properties	Level 3
Saturated Hydraulic Conductivity	Level 3

Soil-Water Characteristic Relationships	Level 3
All Materials physical properties	
Unit weight	Level 2
Poisson's Ratio	Level 3
Other Thermal Properties	Level 3

3.3. Local Calibration Methods

In this research, the general principles and steps suggested by the AASHTO, Guide for the Local Calibration of the Mechanical-Empirical Pavement Design Guide (2010) was followed in this study. To develop a non-biased and precise performance prediction model, the following criteria were considered:

- Minimizing Residual Sum of Square (RSS)

$$RSS = \sum_{i=1}^{n} (D_{Total-i} - d_{Total-i})^2$$

- Eliminating Bias

$$Bias = \sum_{i=1}^{n} (D_{Total-i} - d_{Total-i})$$

where

RSS = Residual Sum of Square

$D_{Total-i}$ =Calculated total rut depth as specified in equation 5

$d_{Total-i}$ =Observed total rut depth

n =Number of rut depth measurements

The total amount of the calculated rut depth would be calculated based on the cumulative ruts which occurs in all of the pavement layers.

$$D_{Total} = D_{AC} + D_{GB} + D_{SG} \quad (6)$$

To develop an optimization model, this study aimed to create a simulating procedure of equation (7) in an Excel file. Since the traffic and temperature exponents β_N and β_T in the AC models have been prefixed, the total rut depth model can be rewritten as the following linear regression model:

$$D_{Total} = \beta_{AC} D_{(AC-Global)} + \beta_{GB} D_{(GB-Global)} + \beta_{SG} D_{(SG-Global)} + \varepsilon \quad (7)$$

Where:

$D_{(AC-Global)}$ =Calculated rut depth in AC layer based on the global model

$D_{(GB-Global)}$ =Calculated rut depth in granular base layer based on the global model

$D_{(SG-Global)}$ = Calculated rut depth in subgrade layer based on the global model

ε = Model error term, following normal distribution $N(\sigma^2, 0)$

To maintain the integrity and validity of the results, effects of zero bias constraint on the produced standard deviation of residual error was evaluated using following methods:

- Method 1: Minimizing the RSS without forcing the bias to zero
- Method 2: Minimizing the RSS by forcing the bias to zero

For each method, optimization analysis was performed based on calculated predicted rut depth for each layer and their correspondent observed values. Using Microsoft Excel Solver, new optimized coefficient values were obtained considering the least residual sum of square, both with and without the constraint of zero bias, for method 1 and 2 respectively. For this study, for the purpose of recalibration and validation, it was decided to split the database into 70% and 30% respectively.

From the total of 63 legitimate sections, 46 sections were chosen randomly for calibration. The remaining 17 sections were used to validate the result of calibration.

3.4. Results and Discussions

3.4.1. Bias and Error of Global Calibration

Based on result of previous research studies it was concluded that rutting model needs to be calibrated for Ontario's conditions. Yet considering following enhancements which differs from previous studies, at the beginning stage of this research, preliminary evaluation on the selected Superpave sections was performed to assess the prediction performance of global rut depth model:

This study used the most recent MTO default parameters to execute the latest version of MEPDG software (V.2.3) on the expanded database included SMA sections.

MEPDG software was executed at 50% reliability to predict rutting values for the lifetime of each section from its latest major rehabilitation up to 2015. To verify the feasibility of the rut-depth global model, statistical analysis was performed based on MEPDG results and respective observed data. That resulted in an average bias equal to 10.32 mm with a standard error of residual equal to 10.63 mm.

Based on the results derived from figure 5 and table 4, measured and predicted rut depth are not from the same population for both models, meaning that the global rut-depth models produce biased prediction for rutting and needs to be recalibrated for Ontario's conditions.

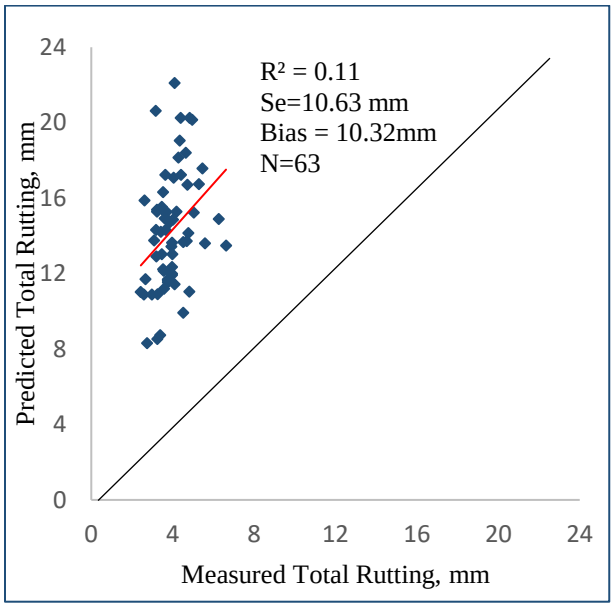

Figure 5. Performance of the default rutting models applied in Ontario's Superpave roads

Table 4. Hypothesis tests of the default model

Null hypothesis Testing	DF	Parameter	Test	Null hypothesis Testing	DF	Parameter
t-test	63	-	27.59	1.99	<0.0001	Rejected
F-test	63	-	14.14	1.51	<0.0001	Rejected

3.4.2. Calibration Results

Table 5. Local calibration results

Coefficient/Parameter	Method 1	Method 2
β_{AC}	1.7009	1.7692
β_{GB}	0.0943	0.0968
β_{SG}	0.2737	0.2787
S_e	1.002 mm	1.006mm
Bias	4.07	0

Based on result derived from table 5, it was concluded that using a constraint of zero bias will not result in significant variation for both calibration coefficients and their respective S_e values. Therefore, using method 2, cross-sectional calibration methodology was performed on 70% of selected Ontario's Superpave pavement sections.

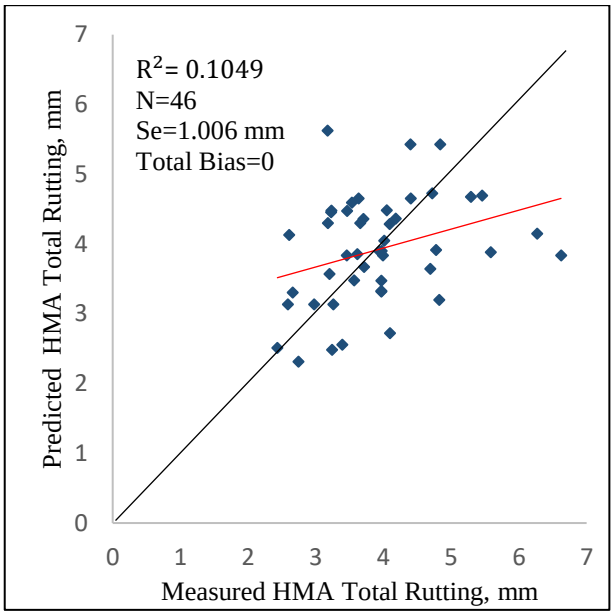

Figure 6. Measured vs. predicted total rut depth (calibration set)

The calibrated models obtained from method 2 were used on the remaining 17 validation databases. The resulting statistics were standard error 0.66 mm and average bias 0.019 mm.

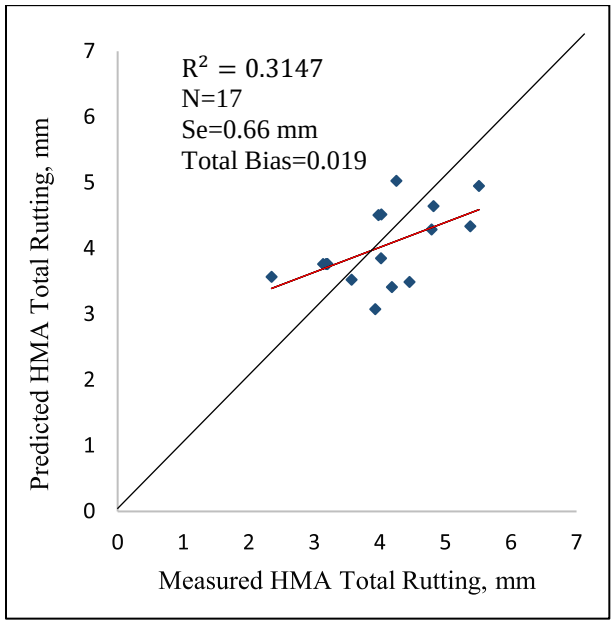

Figure 7. Measured versus predicted total rut depth (validation set)

As verified in figures 6 and 7, the bias and standard error of the residuals for the validation sets were found to be comparable to that from the calibration sets. A further F-test was performed and resulted in a p-value of 6%, which indicated a good validation.

Table 6. Summary statistics of the rutting model calibration

Statistical Parameters	**Global Model based on AASHTO**	**Local Calibration** Performed on 70% of selected Ontario's Superpave pavement sections	**Validation**
R^2	0.577	0.1049	0.3147
Standard Error of the Estimate, S_e	2.717	1.0065(mm)	0.66(mm)
Number of data points, N	334	46	17

Table 7. Comparison of layer contributions between the globally and locally calibrated models

Layers	Global model		Calibrated Model	
	Coefficients	Layer Contribution	Coefficients	Layer Contribution
AC	1	23%	1.7692	19%
GB	1	11%	0.0968	9%
SG	1	66%	0.2787	72%

The final detailed result can be found in tables 6 and 7. Commenting on the accuracy of the layer contribution would be hard since there was no available trench investigation at the time of this study. Figure 8 shows random distribution of residual errors around zero line without any constant decrease or increase trend. From vertical distribution of the scatter, it can be concluded that predicted rut depth falls within two standard error of the estimate of measured values, which indicates a very low bias.

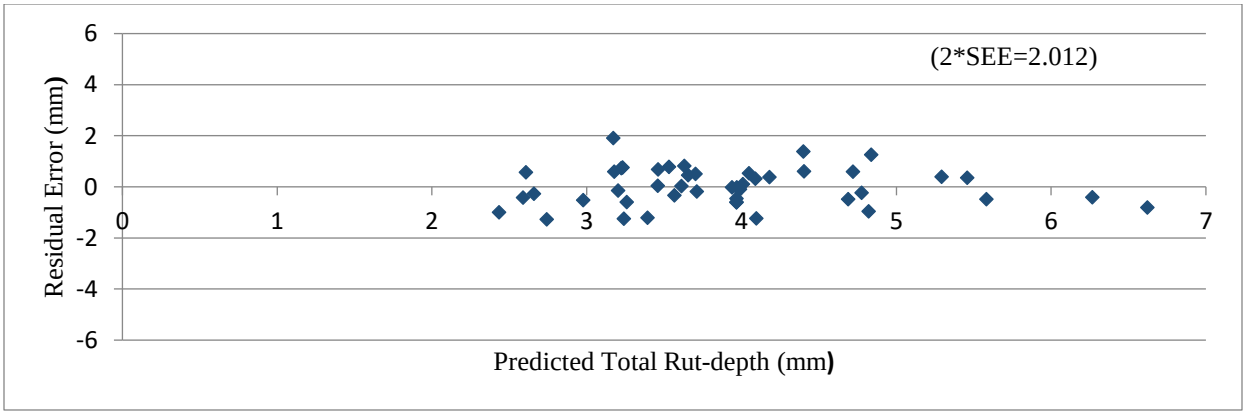

Figure 8. Residual vs. predicted rut depth

CHAPTER 4 IRI MODEL CALIBRATION

4.1. Introduction

The focus of this part of the study was on performing a preliminary local calibration of the current global IRI model for Ontario's Superpave pavements. One important factor that needs to be discussed is that the cracking model calibration has not yet been finalized. For this reason, the IRI study focused on an exploration and presentation of the best calibration method.

4.2. Local Calibration Database

The calibration database has been already discussed in section 3.2. The following discussion focuses on the obtained observed IRI data used within this study. Within this part, sections have been checked for reasonableness and consistency of their distress measurement data, particularly for their IRI_0 values. For each selected section, observed historical IRI measurement data was obtained from Ontario's ARAN database. From the same database used in chapter 3, a total of 52 sections was selected. It is important to understand that for each proposed calibration methods, data selection criteria varied as following:

Method 1 database selection was based on the availability of measured IRI_0 values, therefore only 40 sections were found to be appropriate for its analysis. Method 2 data selection was based on the minimum number of available sections for both overlaid and new/reconstruction conditions, which resulted in the selection of 41 sections. Method 3 did not have any constraints therefore all of the 52 sections were included in its analysis.

4.3. Local Calibration Methods

As mentioned earlier, to perform cross sectional local calibration for IRI model, the general methodology recommended by AASHTO Guide for the Local Calibration of the Mechanical-Empirical Pavement Design Guide (2010) was followed.

To have an accurately predicted IRI, following criteria should be considered:

- Minimizing Residual Sum of Square (RSS)

$$RSS = \sum_{i=1}^{n} (IRI_{Predicted-i} - IRI_{Observed-i})^2$$

- Eliminating Bias

$$Bias = \sum_{i=1}^{n} (IRI_{Predicted-i} - IRI_{Observed-i})$$

MEPDG software consists of the following empirical IRI model:

$$IRI = IRI_0 + C_1(RD) + C_2(FC_{Total}) + C_3(TC) + C_4(SF) \quad (8)$$

The main challenge observed for calibrating IRI model for Ontario's Superpave pavement was selecting an appropriate IRI_0. The initial IRI refers to the smoothness of pavement within six months after completed construction date. In current database, regardless of new or rehabilitated pavements, IRI observed values varies from 0.72 to 1.97 m/km; therefore, using table 8 default parameters for IRI_0 may result in additional variation in the local calibration.

Table 8. Ontario's recommended default IRI (m/km) parameters for treatments and facility type

Treatments	Freeway	Arterial
Hot Mix Overlay 1 lift	1	1
Hot Mix Overlay 2 lifts	0.9	0.9
Mill + Hot Mix Overlay 1 ,2,3 lift	1	1
New or Reconstruction to AC	0.8	Not available

For better understanding the effects of the chosen IRI_0 on the final result, see figure 9 for a comparison between the fluctuation of actual IRI_0 and the default values for both overlay and new pavement sections. Comparing the measured IRI_0 values with their default ones, the standard deviation of the residual was found to be 0.22 m/km and 0.16 m/km for new and overlaid pavement respectively.

In addition, using global IRI model, software was executed for 52 sections using chosen IRI_0 of each model. Subsequently models standard error of residual was calculated. Results can be found in table 9.

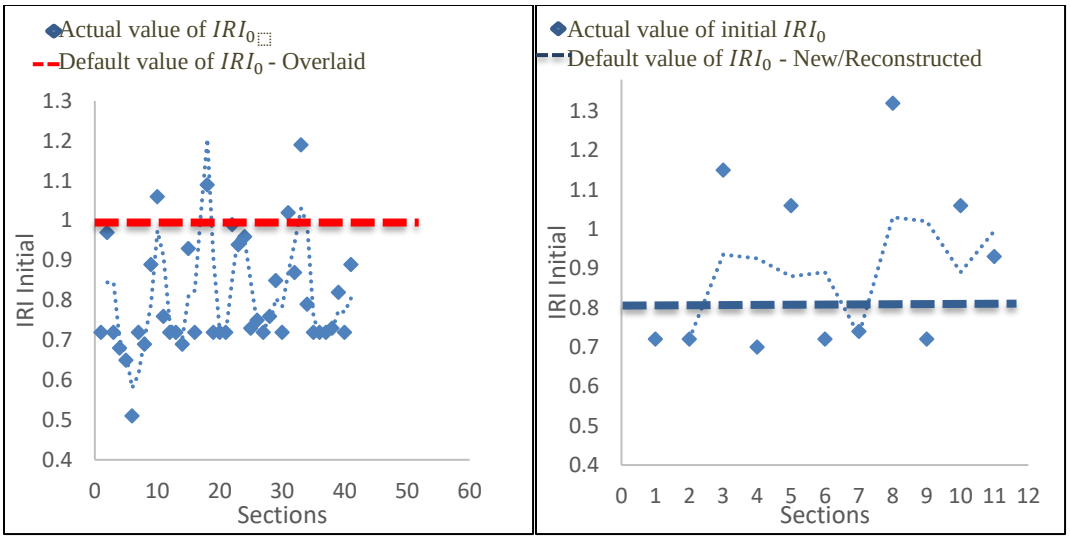

Figure 9. IRI_0 fluctuation - actual vs. default values

Table 9. Comparing S_e values for different IRI_0 using global coefficients

Method	Number of sections	IRI_0	S_e
1	52	0.8(New)-1(Old)	0.42
2	52	0.65	0.31
3	52	From PMS database	0.27

Based on the results derived from figure 9 and table 9, it can be concluded that:

- The standard error of residual of calculated IRI (using default model) ranges from 0.27 to 0.42.
- IRI_0 dominated the variation in the total IRI that is predicted.

Considering the governing effect of IRI_0 on the predicted IRI values, it was decided to explore the best calibration method based on different initial IRI values to be used in the calibration. It is important to understand that the actual IRI_0 value in future design is a policy requirement of the MTO. Each set of coefficient values (C_1, C_2, C_3, C_4) needed to be re-evaluated by using them within a simulated procedure of actual design considering using default parameters for IRI_0 values.

4.3.1. Method 1: Using Actual IRI_0

For the first method, to produce prediction of IRI values, for each section their actual IRI_0 values were used. Actual IRI_0 refers to IRI values from the PMS database in the year of reconstruction, major rehabilitation or construction for the respective section.

Evaluating IRI measured database, for some sections, extensive fluctuation was observed in the trend of their IRI values. That could be a result of either a minor rehabilitation or a non-

accurate measurement. For some sections, even small rehabilitation affected the IRI values to the extent of, their value of IRI in 2015 was smaller compared to the ones in their construction year. To minimize mentioned errors, those sections were eliminated from the final database. In addition, the lack of available information of IRI_0 values for most of SMA sections resulted into their exclusion from the final database of this method.

Split sample method was used to perform a local calibration of the IRI model, with 27 sections (70 % of database) used for calibration. For calibration purposes, software calculation of IRI was simulated within an Excel file. Therefore, for each section, MEPDG software was executed at 50 percent reliability to predict the area of fatigue cracking, average rut and length of transverse cracking within their lifetime considering the latest major rehabilitation up to 2015.

Following information was used to simulate the prediction of IRI values within an Excel file:

For each section, actual IRI_0 value was found from available PMS file. For all sections, using this study rutting model local calibration coefficients, MEPDG software was executed at 50 percent reliability to predict the amount of rutting. For cracking models, their global calibration coefficient values were used.

For each section, from the output of the software, following information was obtained:

For rutting, the amount of rut depth within each layer was obtained. For area of fatigue cracking (FC_{Total}), using the output of the software, the amount of AC top-down fatigue cracking(m/km) were converted into the area by multiplying its software-produced value to 0.3048 m (1 ft). Subsequently for each section, the percentage of its crack within the total lane area was calculated. Finally, for each section, obtained results were added to the values of AC total bottom-up fatigue and thermal reflective cracking (% lane area).

For each section, the amount of mean annual precipitation, mean annual freezing index and clay size particles in subgrade were exported from the output of the software to simulate site factor calculation within the Excel file.

Using above information, the ultimate predicted IRI values were calculated using an Excel simulation model. Subsequently optimization analysis was performed based on calculated predicted IRI and their correspondent observed values. Using Microsoft Excel Solver, new optimized coefficient values were obtained considering the least residual sum of square and zero bias. To validate new obtained coefficients, using local IRI model software was executed on the

remaining sections. F-test (model preciseness) and t-test (bias) was performed on the validation set.

4.3.2. Method 2: Calculating IRI_0 from linear regression

Another method proposed by this study was to determine the best-fit IRI_0 by including it as part of the local calibration coefficients. Determination of IRI_0 should be performed for new/reconstructed and overlaid pavements separately. Considering the limited number of available sections, for this part of the study analysis has been performed only on overlaid sections.

MEPDG software was run for the 41 Superpave sections, using global coefficient values for distress models except for rutting. Using the same method as described before, software procedure in calculating IRI was simulated.

As mentioned previously, a local IRI model needs to be developed considering the least residual sum of square and zero bias. For that, five variables were introduced and solved for $C_1, C_2, C_3, C_4, IRI_0$. Finally, to validate the result, the newly obtained model software was executed on the remaining 12 sections. F-test (model preciseness) and t-test (bias) was performed on the validation set.

4.3.3. Method 3: Using Default IRI_0

The final method presented by this research is based on using Ontario's default values for initial IRI. IRI model was calibrated based on the rate of IRI deterioration caused by distress factors included cracking and rutting.

For this analysis, MEPDG software was executed on total of 52 Ontario Superpave pavement sections considering their default IRI_0 value. From the output of the software, an Excel sheet was created to simulate the calculation of predicted ΔIRI (rate of deterioration). Observed ΔIRI values were calculated based on the PMS 2015 database considering the following equation:

$$\Delta IRI = IRI_{Observed\_at\ year\ 2015} - IRI_{0\_default} \quad (9)$$

The first step was to find the best local calibration coefficients, considering the least residual sum of square and zero bias. To compare and evaluate the final results, a similar procedure to method 1 was performed.

4.4. Results and Discussions

4.4.1. Bias and Error of Global Calibration

To validate the IRI Global model capability in predicting IRI values for Ontario's Superpave pavements, preliminary evaluation was performed on 52 selected pavement sections. For each section, MEPDG software was executed at 50% reliability to predict IRI values for each section service time considering their latest major rehabilitation year up to 2015. Subsequently statistical analysis was performed based on MEPDG results and their respective observed values by using the following null hypothesis tests:

- Null hypothesis 1: To determine if predicted and observed dataset are from the same population, a t-test was performed on IRI experimental database. As a result, p-value founds to be less than 0.05 which indicates that predicted and observed IRI are not from the same population.
- Null hypothesis 2: In addition to bias, global model was studied for its preciseness by performing F-test. As a result, p-value founds to be less than 0.05 which indicates poor preciseness. Based on the results derived from table 10 and figure 10, it was concluded that using global model for prediction of IRI values for Ontario's conditions would be resulted into bias prediction with average bias value of 0.21 m/km. Hence it was decided to perform a local calibration on MEPDG IRI model to reduce bias and to define it with Ontario's conditions.

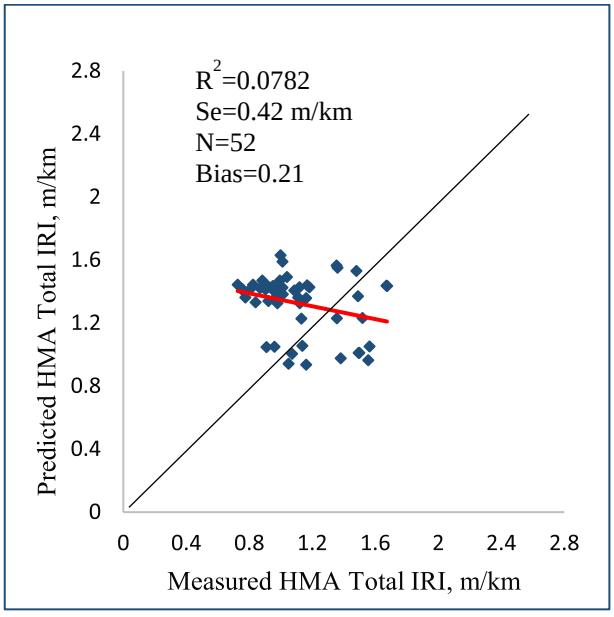

Figure 10. Performance of the default IRI model applied in Ontario's Superpave roads

Table 10. Hypothesis tests of the default model

Null hypothesis Testing	DF	Parameter	Test Statistic	Critical value of the test statistics	p-value	Result
F-test	51	-	1.87	1.59	0.013	Rejected
t-test	51	-	-4.44	2.007	<0.0001	Rejected

4.4.2. Calibration Results

After verifying the existence of bias, observed and predicted values (obtained from the software) were used to determine the most precise calibration coefficients for IRI model considering Ontario's conditions.

4.4.2.1. Method 1 - Using Actual $\mathbf{IRI_0}$

For method 1, 27 sections (70% of database) were chosen randomly from the total of 41 Superpave sections. Calibration analysis was performed considering actual values of IRI_0. This analysis resulted in the following calibration parameters with standard error of 0.13 m/km and average bias equal to 0 (see figure 11).

- C_1, C_2, C_3, C_4 = Local calibration factor for rut depth, fatigue cracking, transverse cracking and site factor found to be equal to 85.83, 0.00013, 0.00026, 0.00193 respectively.

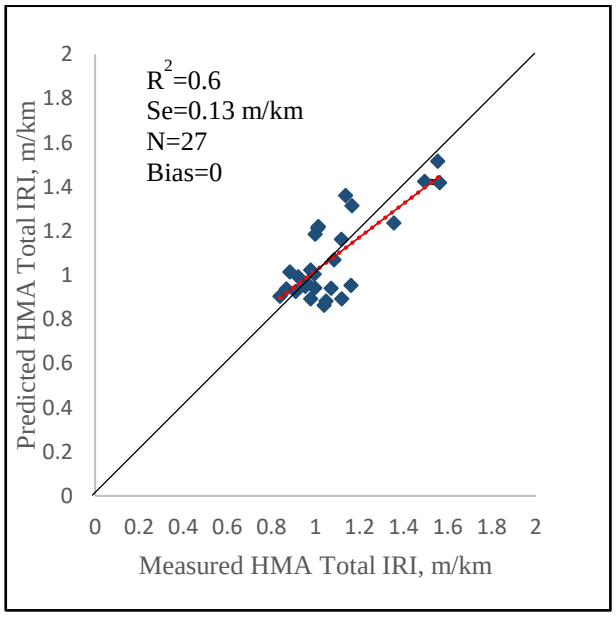

Figure 11. Measured vs. MEPDG-predicted IRI - calibration method 1

The previously calibrated model needs to be validated by executing the new model on the remaining 30% of the research database, therefore the newly obtained calibration factors have been substituted in the MEPDG software to be executed on the remaining 14 sections. Validation analysis resulted into standard error of 0.2 m/km and average bias equal to 0.1 m/km (see figure 12).

Statistical analysis has been performed to assess the accuracy and to determine bias for validation results. Based on information provided in table 11, standard error of the estimated and bias were found to be reasonable. Final results can be found in tables 12 and 13.

Table 11. Hypothesis tests - validation method 1

Null hypothesis testing	DF	Parameter	Test Statistic	Critical value of the test statistics	p-value	Result
t-test	13	-	1.7	2.16	0.06	Accepted
F-test	13	-	1.94	2.57	0.1	Accepted

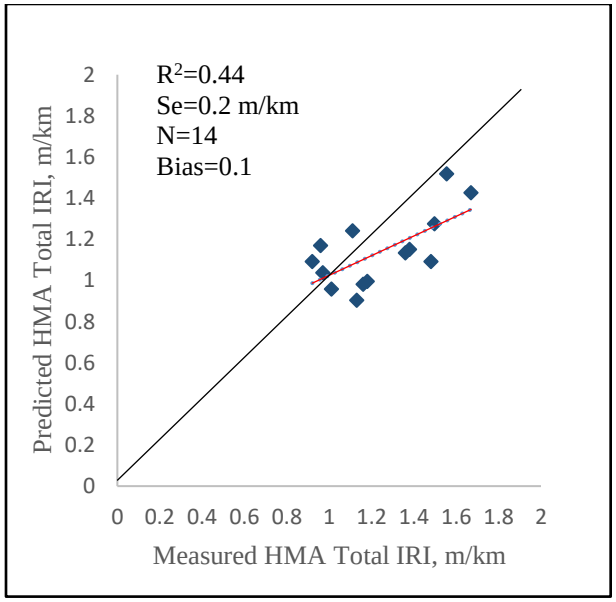

Figure 12. Measured vs. MEPDG-predicted IRI - validation method 1

Table 12.Summary of local calibration effort for Ontario's Superpave pavement IRI model - method 1

Calibration Coefficient	Global Model	Local Calibration -Ontario
C_1	40	85.83
C_2	0.4	0.00013
C_3	0.008	0.00026
C_4	0.015	0.00193

Table 13. Summary of statistical parameters: local calibration efforts for Ontario's Superpave pavement IRI model - method 1

Statistical Parameters	Global model	Local calibration Performed on 70% of selected Ontario's Superpave pavement sections	Validation
R^2	0.56	0.6	0.44
Standard Error of the Estimate, S_e	0.14(m/km)	0.13(m/km)	0.2(m/km)
Number of sections	1926	27	14

Figure 13 represents an arbitrary distribution of residual errors around zero line, from vertical distribution of the scatter, it can be concluded that predicted IRI mostly falls within two standard error of the estimate, which indicates an acceptable bias.

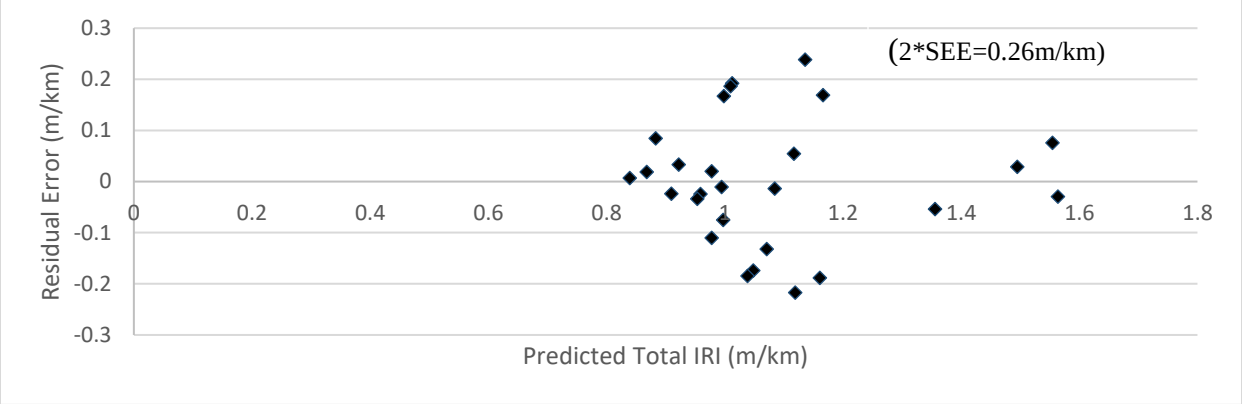

Figure 13. Residual vs. predicted IRI - method 1

4.4.2.2. Method 2 - Calculating **IRI_0** from linear regression

For the calibration part, 29 sections were chosen randomly from overall 41 of Superpave sections. Calibration analysis was performed considering IRI_0 as one of the local calibration coefficients. Based on information provided in figure 14 this analysis resulted into zero bias and standard error of residual equal to 0.26 m/km with following calibration coefficients:

- $C_1, C_2, C_3, C_4, IRI_0$=Calibration factor for rut depth, fatigue cracking, transverse cracking, site factor and IRI_0, values are equal to 33.87, 0.39, 0.0026, 0.02, 0.65 respectively.

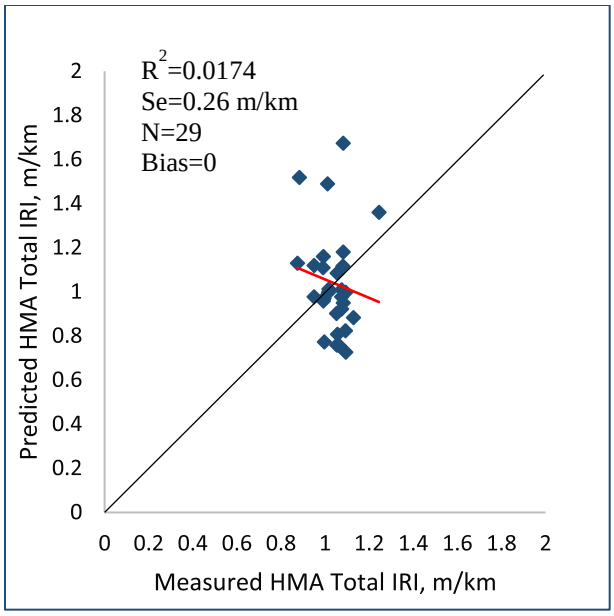

Figure 14. Measured vs. MEPDG-predicted IRI - calibration method 2

To verify the result, MEPDG software was executed on the remaining 12 sections using the newly obtained coefficient values. As shown in table 14 and figure 15, using new calibration coefficients and IRI_0 values, will be resulted into precise model with negligible average bias equal to 0.06m/km. Final detailed results can be found in table 15 and 16 and figure 14.

Figure 16 shows arbitrary distribution of residual errors around zero line, vertical distribution of the scatter shows the predicted IRI values are mostly falls within two standard error of the estimate, which indicates an acceptable bias.

Table 14. Hypothesis tests – validation method 2

Null hypothesis Testing	DF	Parameter	Test Statistic	Critical value of the test statistics	p-value	Result
F-test	11	-	1.39	2.8	0.3	Accepted
t-test	11	-	0.64	2.2	0.53	Accepted

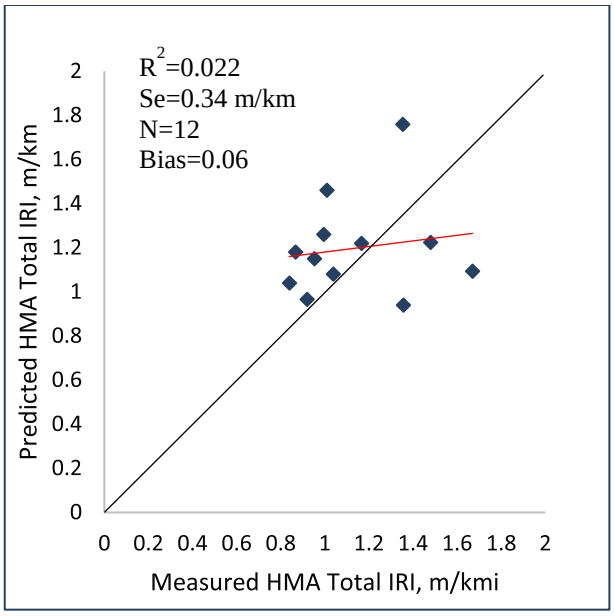

Figure 15. Measured vs. MEPDG-predicted IRI - validation method 2

Table 15. Summary of local calibration efforts for Ontario's Superpave pavement IRI model

Calibration Coefficient	Global Model	Local Calibration –Ontario
C_1	40	33.87
C_2	0.4	0.39
C_3	0.008	0.0026
C_4	0.015	0.02
IRI_0	1	0.65

Table 16. Summary of statistical parameters- local calibration efforts for Ontario's Superpave pavement IRI model - method 2

Statistical Parameters	Global model	Local calibration Performed on 70% of selected Ontario's Superpave pavement sections	Validation
R^2	0.56	0.0174	0.022
Standard Error of the Estimate, S_e	0.14(m/km)	0.26(m/km)	0.34(m/km)
Number of sections,	1926	29	12

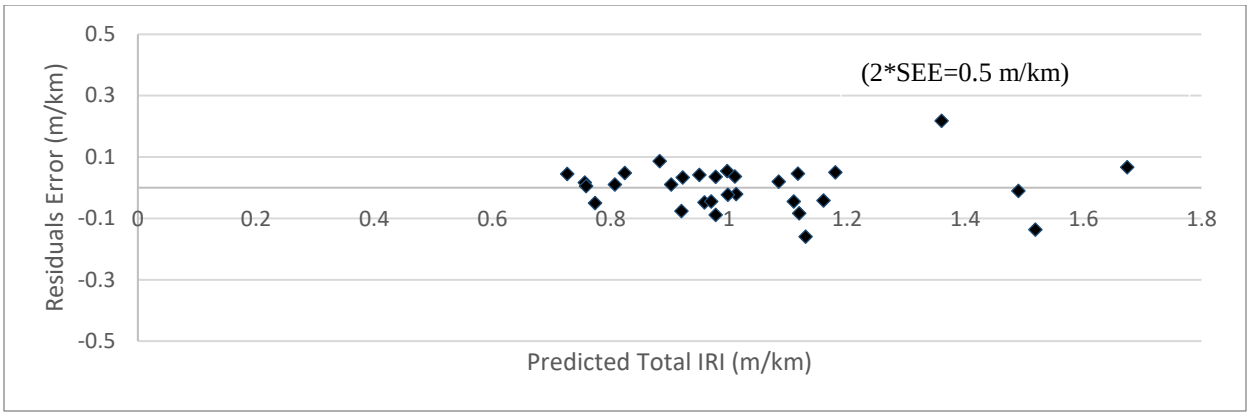

Figure 16. Residual vs. predicted IRI - method 2

4.4.2.3. Method 3 - Using Default $\mathbf{IRI_0}$

Optimization analysis was performed using calculated predicted ΔIRI results and their respective observed values.

Using Excel Solver, new optimized coefficient parameters was obtained by generating least residual sum of square value and setting constraint of bias to be equal to zero. Based on table 17 and figure 17, optimization process led to reduced standard error equal to 0.27 mm. Unfortunately, zero values for C_1, C_2, C_3 coefficients were obtained, which could not be considered as an acceptable result. Hence, subsequent steps were not followed for this method. Table 18 summarized the results of all three methods used within this section.

Table 17. Summary of local calibration efforts for Ontario's Superpave pavement IRI model - method 3

Calibration Coefficient	Global Model	Local Calibration –Ontario
C_1	40	0
C_2	0.4	0
C_3	0.008	0
C_4	0.015	0.025

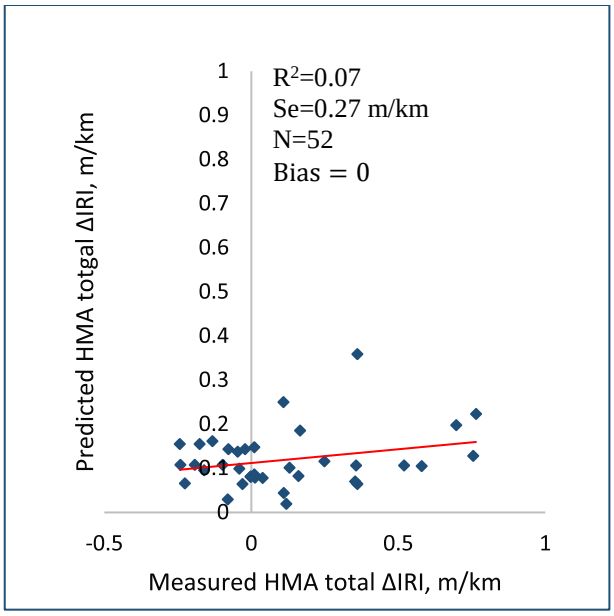

Figure 17. Measured versus MEPDG predicted ΔIRI – calibration method 3

Table 18. Summary of local calibration efforts for Ontario's Superpave pavement IRI model

Parameter	**Method**		
	1	**2**	**3**
C_1	85.83	33.87	0
C_2	0.00013	0.39	0
C_3	0.00026	0.0026	0
C_4	0.00193	0.02	0.025
R^2	0.6	0.0174	0.07
S_e	0.13 m/km	0.26 m/km	0.27 m/km

To present the best calibration method it is important to understand that for future design the value of IRI_0 should be based on the latest MTO default parameters. Therefore, coefficients obtained from each method need to be re-evaluated by simulating the actual design procedure when using IRI_0 default parameters.

In order to simulate future design conditions, software was executed in two separate rounds on the total of 52 sections. The first round used method 1 coefficient values and second round used method 2 coefficient values. It is important to understand that for both rounds, input values for IRI_0 were based on the current MTO default parameters. For each simulated design

method, based on their predicted IRI results and respective observed ones, standard deviations of residual were calculated. Based on the results shown in table 19, method 1 would be recommended as the best calibration method by this study.

Table 19. Simulated future design conditions - value of S_e

Calibration Coefficient		
	Method 1	**Method 2**
S_e	0.30 m/km	0.40 m/km

CHAPTER 5 SUMMARY, CONCLUSIONS AND RECOMMENDATIONS

This chapter summarizes and derives conclusions from works performed by this study on the local calibration of the IRI and rutting models. Finally, based on conclusions in this chapter, recommendations for the enhancement of this study for future research will be presented.

5.1. Summary

The focus of the current study was to perform a local calibration of rutting and IRI models, two distress models of the MEPDG, for Ontario's Superpave sections.

The literature review on rutting models illustrated the need to further enhance the result of local calibration for rutting models. In addition, as a result of the ongoing use of SMA materials within the new design, an expanded database was built that included new SMA sections. A cross-sectional calibration was performed based by the least squares method, which resulted in a more precise and reasonable result compared to global and current locally calibrated models.

For the IRI model, due to the absence of local coefficient values for cracking models, the main focus was to introduce the best method of achieving local coefficient values.

5.2. Conclusions

The conclusions drawn from this study are as follows:

Using global models for both rutting and IRI results in imprecise and mostly overestimated prediction results. Performing a cross-sectional local calibration on the rutting model resulted in the following calibration parameters: $\beta_{AC} = 1.7692, \beta_{GB} = 0.0968, \beta_{SG} = 0.2787$ with layer contributions of 19%, 9% and 72%, respectively. This resulted in a reduced residual standard deviation equal to 1 mm, a significant improvement compared to previous studies. Therefore, the calibration parameters obtained for rutting models can be used as level three rutting model calibration parameters for both new and rehabilitated Superpave pavements within Ontario's conditions.

To perform a local calibration for the IRI model, the following methods are proposed by this study:

- Method 1 - Using actual observed IRI_0 values
- Method 2 - Including IRI_0 as one of the coefficient parameters and solving for it
- Method 3 - Using Ontario's default parameter for IRI_0 values

Based on the results of this study, it was concluded that using method 1 coefficient values would lead to a more precise prediction of IRI in future designs and hence was found to be the best approach to be used for future calibrations.

5.3. Recommendations

More studies need to be conducted to finalize the local calibration of the MEPDG distress and performance models. Below are the major recommendations for future studies.

- The observed rut depth and IRI values available for this study did not reach the MTO thresholds. To enhance local calibration studies, it is recommended that the updating of local calibration of the rutting model be continued as new rutting observation data that reaches or exceeds the design thresholds are made available.
- The calibrated rutting models in this study have resulted in a contribution to rutting by various pavement layers similar to that in the global calibration, which can be further traced back to the AASHO test results of the 1960s. Trench investigation is recommended for a final validation of the global and local calibration results.
- The IRI_0 value is an important design policy parameter to be determined by the MTO. Further analysis using existing initial IRI data in PMS and local calibration is recommended to determine the optimal IRI_0 value for future design. The optimal IRI_0 value is not necessarily the mean value of the IRI_0 database; rather, sensitivity analyses need to be conducted to confirm the impact on initial capital and construction administration costs.
- After a successful calibration of the cracking models, a full-course local calibration of the IRI model following the methods proposed in this study is recommended.

APPENDIX A: PAVEMENT SECTIONS, STRUCTURES, AND MATERIALS

Table A-1 Selected Superpave sections used in the study

Section Number	ID	From _LHRS	To-LHRS	Region
1	77	12020+1.3	12036+0.0	Western
2	78	12036+0.0	12038+0.0	Western
3	105	13465+0.0	13515+0.0	Central
4	114	13640+2.1	13650+2.46	Western
5	197	14612+0.88	14620+6.0	Western
6	206	14612+0.88	14620+6.0	Western
7	253	16590+0.00	16600+0.00	Western
8	437	20020+3.820	20035+0.800	Eastern
9	587	24030+0.000	24030+12.970	Western
10	589	24050+5.2	24060+0.10	Western
11	600	24142+0.1	24142+13.0	Western
12	670	27816+0.0	27822+0.0	Central
13	673	27816+0.0	27822+0.0	Central
14	697	29580+2.800	29590+3.900	Central
15	698	29590+3.900	29590+11.300	Eastern
16	727	33240+0.000	33240+7.850	Eastern
17	728	33240+7.850	33250+1.600	Eastern
18	826	38630+0.24	38635+0.0	Central
19	976	46969+0.000	46972+0.000	Northeastern
20	977	46972+0.000	46977+6.200	Northeastern
21	1001	46969+0.000	46972+0.000	Northeastern
22	1052	47603+0.0	47607+0.0	Central
23	1240	48335+0.0	48342+1.0	Western
24	1246	48255+1.65	48270+1.0	Central
25	1247	48250+1.65	48255+1.65	Central
26	1248	48255+1.65	48270+1.0	Central
27	1255	48335+0.0	48342+1.0	Western
28	1260	48250+1.65	48255+1.65	Central
29	1261	48255+1.65	48255+1.65	Central
30	1287	48652+1.326	48660+2.465	Central
31	764	34320+0.000	34330+0.800	Northeastern

32	952	46130+9.900	46140+0.000	Northeastern
33	107	13570+5.90	13580+1.00	Central
34	109	13585+0.300	13585+3.244	Central
35	115	13650+2.46	13650+11.44	Western
36	144	14024+0.000	14040+0.000	Eastern
37	159	14200+8.000	14210+0.800	Eastern
38	166	14270+0.000	14270+8.700	Eastern
39	240	16460+0.000	16460+8.270	Central
40	271	17360+3.900	17380+0.000	Northeastern
41	760	34120+0.000	34133+4.771	Northeastern
42	791	35550+14.300	35560+1.100	Northeastern
43	1139	47603+0.0	47607+0.0	Northeastern
44	1331	49500+0.000	49540+0.000	Eastern
45	1332	49540+0.000	49550+0.000	Eastern
46	1-SMA	13605+0.1	13605+1.2	Western
47	2-SMA	13605+1.2	13605+1.9	Western
48	3-SMA	13605+1.9	13605+2.8	Western
49	4-SMA	13605+2.8	13607+0.1	Western
50	5-SMA	10131+0.000	10135+0.800	Central
51	6-SMA	10100+0.000	10105+1.603	Central
52	7-SMA	46820+0.5	46823+0.5	Central
53	8-SMA	47820+1	47823+0.9	Western
54	9-SMA	47805+0.9	47815+3	Western
55	10-SMA	47760+1	47760+12.2	Western
56	11-SMA	47760+12.2	47784+1	Western
57	12-SMA	47784+1	47786+1	Central
58	13-SMA	48315+0.2	48315+3.3	Central
59	14-SMA	48315+0.2	48315+3.3	Central
60	15-SMA	47810+0.9	47815+1	Western
61	16-SMA	13600+0.1	13600+3.2	Western
62	17-SMA	13600+5.2	13605+0.1	Western
63	18-SMA	13600+3.3	13600+4.3	Western
64	19-SMA	10128+0.000	10131+0.000	Central

Table A-2- Material and structural information for the selected Superpave sections

Section Number	ID	Service Age (years)	First Layer		Second layer		Third Layer		Forth Layer		Fifth Layer		Subgrade Soil	Resilience Modulus, Mr (MPa)
			Material	Thickness (mm)	Material	Thickness (mm)	Material	Thickness (mm)	Material	Thickness (mm)	Material	Thickness (mm)		
1	77	10	SP 12.5 FC2	40	SP 19	60	SP 19	70	Old Granular Base	200	Old Granular Subbase	150	CL	36
2	78	10	SP 12.5 FC2	40	SP 19	60	SP 19	70	Old Granular Base	200	Old Granular Subbase	150	CL	36
3	105	12	SP 12.5 FC2	40	SP 19	50	SP 19	110	Old Granular Base	150	Old Granular Subbase	550	CL-ML	30
4	114	7	SP 12.5 FC1	40	SP 19	50	SP 19	50	Granular A	225			SM	35
5	197	9	SP 12.5 FC2	40	SP 19	60	SP 19	60	Pulverized Layer	300	Old Granular BIII	300	SM-SC	30
6	206	9	SP 12.5 FC2	40	SP 19	60	SP 19	60	Pulverized Layer	300	Old Granular BIII	300	SM-SC	30
7	253	10	SP 12.5 FC1	50	SP 19	100	Pulverized Layer	200	Old Granular Subbase	300			SM	35
8	437	12	SP 12.5 FC1	40	SP 19	60	SP 19	60	Granular A	150	Granular B1	450	CH	20
9	587	6	SP 12.5	50	CIR	110	Old Granular Base	180	Old Granular Subbase	800			SM	40
10	589	11	SP 12.5	60	SP 19	75	Pulverized Layer	320	Old Granular Subbase				CL-ML	30
11	600	5	SP 12.5	40	SP 19	110	Pulverized Layer	100	Old Granular Base	200	Old Granular Subbase	560	CI-CL	35
12	670	11	SP 12.5 FC2	40	SP 19	50	HL-8	130	Old Granular Base	550			SM	35
13	673	10	SP 12.5 FC2	40	SP 19	50	HL-8	130	Old Granular Base	550			SM	35
14	697	7	SP 12.5	40	SP 19	50	Granular A	200					SM	80
15	698	8	SP 12.5	40	SP 19	50	Pulverized Layer	200	Granular A	190	Old Granular Subbase	150	SM	80
16	727	6	SP 12.5	50	HL-8	150	Old Granular Base	145	Pulverized Layer	150			SM	80
17	728	6	SP 12.5	50	HL-8	150	Old Granular Base	145	Pulverized Layer	150			SM	80
18	826	5	SP 12.5 FC2	40	SP 19	110	EAS	130	Old Granular Base	290	Old Granular Subbase	240	CL-ML	25
19	976	7	SP 12.5 FC2	40	SP 19	50	CIR	100	HL-4	40	Granular A	420	CL-ML	35
20	977	9	SP 12.5 FC2	40	SP 19	50	CIR	100	HL-4	40	Granular A	420	CL-ML	35
21	1001	15	SP 12.5 FC2	40	SP 19	50	CIR	100	HL-4	170	Granular A	540	CL-ML	70
22	1052	6	SP 12.5 FC2	40	SP 19	50	HL-3	160	Old Granular Base	320	Old Granular Subbase	550	CL-ML	30
23	1240	9	SP 12.5 FC2	40	SP 19	100	HL-4	120	Granular A	225	Granular B1	375	SM	40
24	1246	11	SP 12.5 FC2	40	SP 19	40	HDB	200	Old Granular Base	300	Old Granular Subbase	300	CI	35
25	1247	2	SP 12.5 FC2	40	SP 19	40	HDB	200	Old Granular Base	300	Old Granular Subbase	300	CL	35
26	1248	11	SP 12.5 FC2	40	SP 19	40	HDB	200	Old Granular Base	300	Old Granular Subbase	300	CI	35
27	1255	9	SP 12.5 FC2	40	SP 19	100	HL-4	120	Granular A	225	Granular B1	375	SM	40
28	1260	2	SP 12.5 FC2	40	SP 19	40	HDB	200	Old Granular Base	300	Old Granular Subbase	300	CL	35
29	1261	2	SP 12.5 FC2	40	SP 19	40	HDB	200	Old Granular Base	300	Old Granular Subbase	300	CI	35
30	1287	8	SP 12.5 FC2	40	SP 19	60	SP 25	100	Granular A	450			CL	35
31	764	7	SP 12.5	50	Pulverized Layer	200	Old Granular Base	120	Old Granular Subbase	600			CL-ML	35
32	952	11	SP 12.5	50	EAS	150	Old Granular Base	50	Old Granular Base	115	Old Granular Subbase	612	SM	42
33	107	16	SP 12.5 FC2	40	SP 19	50	HL3	110	Old Granular Base(BI)	700			CI-CL	30
34	109	10	SP 12.5 FC2	40	SP 19	50	HL3	110	Old Granular Base	700			CI-CL	30
35	115	17	SP 12.5 FC1	40	SP 19	50	SP 19	50	Granular A	225			SM	35
36	144	11	SP 12.5 FC2	40	SP 19	60	SP 19	70	Granular O	150	Granular B2	450	CI-CL	30
37	159	7	SP 12.5 FC1	60	CIR	70	HL-4	90	Old Granular Base	315	Old Granular Subbase	300	SM	50
38	166	11	SP 12.5 FC1	40	SP 19	50	SP 19	50	Pulverized Layer	200	Old Granular Subbase	400	SM	30
39	240	6	SP 12.5 FC2	40	SP 19	50	SP 19	50	Old Granular Base	500			CL-ML	30
40	271	7	SP 12.5	40.0	SP 19	50	CIR	110	HL-4	140	Granular A/Granular B1	200/700	CL-ML	40
41	760	7	SP 12.5	40	SP 19	50	EAS	175	Granular A	100	Old Granular Subbase	625	CL-ML	45
42	791	9	SP 12.5 FC1	100	SP 25	200	Granular	150	Granular B	150			CL-ML	90
43	1139	17	SP 12.5	40	SP19	50	HL3	160	Old Granular Base	320	Old Granular Subbase	550	CL-ML	30

Section Number	ID	Service Age (years)	First Layer		Second layer		Third Layer		Forth Layer		Fifth Layer		Subgrade Soil	Resilience Modulus, Mr (MPa)
			Material	Thickness (mm)	Material	Thickness (mm)	Material	Thickness (mm)	Material	Thickness (mm)	Material	Thickness (mm)		
44	1331	5	SP 12.5 FC2	40	SP 19	100	HDB	40	HL-4	185	Old Granular Base	225	CL-ML	31
45	1332	9	SP 12.5 FC2	40	SP 19	100	HDB	40	HL-4	185	Old Granular Base	225	CL-ML	31
46	1-SMA	3	SMA (70-28)	50	SP 19	60	SP 19	50	Old Granular Base	260	Old Granular Subbase	500	SC	33
47	2-SMA	3	SMA (70-28)	50	SP 19	50	SP 19	60	Old Granular Base	260	Old Granular Subbase	450	SC	33
48	3-SMA	3	SMA (70-28)	50	SP 19	50	SP 19	110	Old Granular Base	260	Old Granular Subbase	450	SC	33
49	4-SMA	3	SMA (70-28)	50	SP 19	50	SP 19	110	Old Granular Base	260	Old Granular Subbase	450	SC	33
50	5-SMA	6	SMA (70-28)	40	SP 19	160	SP 25	100	Granular A	150	Granular B1	600	CL-ML	30
51	6-SMA	6	SMA (70-28)	40	SP19	180	Granular A	150	Granular B1	600			CL-ML	30
52	7-SMA	5	SMA (70-28)	40	SP19	50	HL-3	200	Granular A	150	Old Granular Subbase	450	CI-CL	30
53	8-SMA	9	SMA (64-28)	40	SP19	100	SP 25	200	Old Granular Base	150	Old Granular Subbase	550	CL	30
54	9-SMA	9	SMA (64-28)	50	Existing HDBC	70	HL-4	140	Old Granular Base	260	Old Granular Subbase	550	CL	30
55	10-SMA	7	SMA (70-28)	40	SP19	70	SP 25	160	Granular A	150	Granular B1	750	CL	25
56	11-SMA	7	SMA (70-28)	40	SP19	70	SP 25	160	Granular A	150	Granular B1	750	CL	25
57	12-SMA	7	SMA (70-28)	40	SP19	70	SP 25	160	Granular A	150	Granular B1	750	CL	25
58	13-SMA	9	SMA (70-28)	40	SP19	70	HL-3	120	Old Granular Base	150	Old Granular Subbase	720	CL-ML	30
59	14-SMA	9	SMA (70-28)	40	SP19	70	HL-3	120	Old Granular Base	150	Old Granular Subbase	720	CL-ML	30
60	15-SMA	9	SMA (64-28)	50	Existing HDBC	70	HL-4	140	Old Granular Base	260	Old Granular Subbase	550	CL	30
61	16-SMA	3	SMA (70-28)	50	SP19	50	SP19	110	Old Granular Base	150	Old Granular Subbase	415	SC	33
62	17-SMA	3	SMA (70-28)	50	SP19	50	SP19	110	Old Granular Base	260	Old Granular Subbase	450	SC	33
63	18-SMA	3	SMA (70-28)	50	SP19	50	SP19	110	Old Granular Base	260	Old Granular Subbase	450	SC	33
64	19-SMA	4	SMA (70-28)	40	SP19	100	SP 25	140	Granular A	150	Granular B1	450	CL-ML	30

APPENDIX B: CLIMATE, TRAFFIC AND OTHER INPUTS USED IN AASHTOWARE PAVEMENT ME DESIGN

Table B-1 Climate input information used for this study

Inputs	Value
Location	
Longitude (℃)	Project specific
Latitude (℃)	
Elevation (m)	
Ground water(GWT)	
Depth of water table (m)	6.1(Ontario's default parameter)
Climate	
Number of wet days	Project specific
Freezing index(℃-day)	Project specific
Mean annual precipitation	Project specific
Mean annual air temperature (℃)	Project specific
Average annual number of freeze/thaw cycles	Project specific
Hourly climate data	Project specific
Climate Station	Project specific
Monthly temperature	Project specific

Table B-2 Traffic input values used for this study

Inputs	Value
Two-way AADTT	Project detail
Number of Lanes	Project detail
Percent of Truck in design direction	50 %
Percent of Truck in design lane	Table 5-MTO default parameters for AASHTOWare ME design-2016
Operational Speed	Project detail
Vehicle class distribution	Project detail
Growth rate	Project detail
Monthly adjustment	1
Axle per truck	Project detail
Average axle width	2.6(m)
Dual tire spacing	305(mm)
Tire pressure	827.4 (kPa)
Tandem Axle Spacing	1.5(m)
Tridem Axle Spacing	1.7(m)
Quad Axle Spacing	1.3(m)
Average Spacing for short axles	3.658(m)
Average Spacing for medium axles	4.572(m)
Average Spacing for long axles	5.486(m)
Percent Truck with short/medium/long axles	33/33/34
Mean Wheel Location	460(mm)
Traffic Wander Standard Deviation	254(mm)
Design Lane Width	Project detail

Table B-3 Material input values for ac and unbound materials

Input Group	Inputs		Value
Asphalt layers	Material type and thickness		Project specific
	Mixture volumetric	Air void (%)	Refer to table C-1
		Effective binder content (%)	
		Unit weight (Kg/m3)	
		Poisson ratio	0.35 (OGDL, 0.4)
	Mechanical properties	Asphalt binder	Table B-1
		Creep compliance (1/GPa)	Level-3 software default values
		Dynamic modulus	
		G* predictive model	
		Reference temperature (℃)	21.1℃
		Indirect tensile strength at –10 ℃ (MPa)	Model calculated values
	Thermal properties	Heat capacity (J/(Kg·°K))	963
		Thermal conductivity (W/m·°K)	1.16
		Thermal contraction	Model calculated values
Unbound layers	Material type and thickness		Project specific
	Coefficient of lateral earth pressure		0.5
	Poisson ratio		0.35
	Resilient modulus (MPa)		Table C-2
	Gradation and other engineering properties		Table C-2

APPENDIX C: MTO DEFAULT PARAMETERS FOR AASHTOWARE PAVEMENT ME DESIGN

This section will provide information on the latest updated default parameter introduced by MTO in 2016 to be used as default parameter for input level 3 in MEPDG software.

Table C-1 Typical Superpave and SMA materials and their properties (MTO 2016)

Asphalt Layers		**SP 12.5**	**SP 19.0**	**SP 25.0**	**SMA 12.5**
Thickness (mm)		Project specific			
Mixture Volumetric					
Unit Weight (kg/m^3)		See Note 1	2460	2469	See Note 1
Effective Binder Content - by Volume (%)		11.8	11.2	10.4	14.6
Air Voids (%) [Note 2]		7.0			
Poisson's Ratio [Note 3]		0.35 for existing HMA (select calculated for new HMA)			
Mechanical Properties					
Dynamic Modulus		"Input level: 3" selected			
Aggregate Gradation	% Passing the 19 mm Sieve	100 %	96.9 %	89.1 %	100.0 %
	% Passing the 9.5 mm Sieve	83.2 %	72.5 %	63.3 %	73.1 %
	% Passing the 4.75 mm Sieve	54 %	52.8 %	49.3 %	29.7 %
	% Passing the 75 □m Sieve	4 %	3.9 %	3.8 %	9.3 %
G Star Predictive Model		"Use viscosity based model (nationally calibrated)" selected			
Reference Temperature		21.1 ^{0}C			
Asphalt Binder [Note 4]		PG 64-28	PG 58-28	PG 58-28	PG 70-28
Indirect Tensile Strength – 10 deg.C (MPa)		Calculated			
Creep Compliance (1/GPa)		"Input level: 3" selected			
Thermal					
Thermal Conductivity (Watt/Meter-Kelvin)		1.16			
Heat Capacity (joule/Kg-Kelvin)		963			
Thermal Contraction		Calculated			

Note 1: For SP 12.5, the unit weight is 2,460 kg/m^3. For SP 12.5FC1, FC2 and SMA 12.5, unit weight varies from different regions: Central and North regions – 2,520 kg/m^3; East region – 2,390 kg/m^3; West region – 2,530 kg/m^3

Note 2: For existing HMA layers, should use measured in-situ air voids.

Note 3: For new HMA mixtures, use calculated Poisson's ratio by expanding the row on 'Poisson's ratio' and set to 'true'. For the row on 'Is Poisson's Ratio calculated?' Refer to Mechanistic-Empirical Pavement Design Guide table 11-3 for other reference temperatures and open-graded HMA Poisson ratios.

Note 4: Typical PG shown only; PGAC varies based on locations and traffic loading conditions. Refer to MTO Superpave Guide to select the proper PGAC grade.

Table C-2 Ontario typical granular material properties (MTO 2016)

Unbound		**Granular A**	**Granular B-I**	**Granular B-II**	**Granular B-III**	**Granular O**
Layer Thickness (mm)		Project specific				
Poisson's Ratio		0.35				
Coefficient of Lateral Pressure		0.5				
Modulus						
Resilient Modulus		250	150	200	150	200
Sieve						
Gradation and other engineering properties						
Aggregate Gradation (percent passing)	75 µm	5	4	5	4	2.5
	300 mm	13.5	33.5	13.5	18.5	-
	1.18 mm	27.5	55	25	35	7.5
	4.75 mm	45	60	37.5	55	32.5
	9.5 mm	61.5	-	-	66	60
	13.2 mm	77.5	-	-	-	70
	19.0 mm	92.5	-	-	-	87.5
	25 mm	100	75	75	75	97.5
Liquid Limit		6	11	11	11	6
Plasticity Index		0				
Is layer compacted		Yes				
Maximum dry unit weight		Calculated				
Saturated hydraulic conductivity		Calculated				
Specific gravity of solids		Calculated				
Optimum gravimetric water content (T)		Calculated				

Table C-3 Ontario typical subgrade properties (MTO 2016)

		Subgrade Type								
		CL	**CI**	**CH**	**CL-ML**	**ML**	**MI**	**MH**	**SM**	**SC**
Unbound										
Layer Thickness (mm)		Semi-infinite								
Poisson's Ratio		0.45 (saturated) 0.2 (unsaturated)			0.325				0.3 (dense) 0.15 (coarse-grained) 0.25 (fine-grained)	
Coefficient of Lateral Pressure (k_0)		0.65 (very stiff and hard residual) 0.72 (medium stiff)			0.73				0.68	
Modulus										
Resilient Modulus (MPa)		Within current study based on project specific								
Gradation and other engineering properties										
Aggregate Gradation (percent passing)	0.002 mm	30	37	60	16	11	25	40	8	13
	0.075 mm	80	88	92	84	74	82	84	29	32
	0.180 mm	84	92	94	89	86	91	91	58	48
	0.425 mm	91	95	96	92	91	95	96	72	56
	2.00 mm	95	98	98	96	95	98	99	84	86
	4.75 mm	97	99	99	98	96	100	100	90	93
	9.5 mm	99	100	100	99	100	100	100	94	100
	12.5 mm	100	100	100	100	100	100	100	97	100
	19.0 mm	100	100	100	100	100	100	100	98	100
	25.0 mm	100	100	100	100	100	100	100	100	100
Liquid Limit		26	41	67	22	26	42	53	18	22
Plasticity Index		12	21	43	6	3	15	21	4	10
Is layer compacted		Yes								
Maximum dry unit weight (kg/m^3)		Calculated								
Saturated hydraulic conductivity (m/hr)		Calculated								
Specific gravity of solids		Calculated								
Optimum gravimetric water content (T)		Calculated								

Table C-4 Ontario typical Marshal Mix properties (MTO 2016)

Asphalt Layers		**DFC**	**HDBC**	**MDBC**	**HL-1**	**HL-2**	**HL-3**	**HL-4**	**HL-6**	**HL-8**
Thickness (mm)		Project specific								
Mixture Volumetric										
Unit Weight (kg/m3)		2520	2460	2500	2520	2410	2520	2480	2460	2460
Effective Binder Content - by Volume (%)		12.4	10.9	12.3	12.4	14.2	12.4	12.2	10.9	10.9
Air Voids (%) Note 1		3.5	4	4	4	5	4	4	4	4
Poisson's Ratio		0.35								
Mechanical Properties										
Dynamic Modulus		Calculated								
Aggregate Gradation	% Passing the 19 mm Sieve	100	97	97	100	100	100	100	97	97
	% Passing the 9.5 mm Sieve	82.5	63	63	82.5	100	82.5	72	72	63
	% Passing the 4.75 mm Sieve	52.5	43.5	40	55	92.5	55	53.5	53.5	42.5
	% Passing the 75 □m Sieve	2.5	3	3	2.5	5.5	2.5	3	3	3
G Star Predictive Model		"Use viscosity based model (nationally calibrated)" selected								
Reference Temperature		21.1 ºC								
Asphalt Binder		Penetration Grade Note 2								
Indirect Tensile Strength – 10 deg.C (MPa)		Calculated								
Creep Compliance (1/GPa)		"Input level: 3" selected								
Thermal										
Thermal Conductivity (watt/meter-Kelvin)		1.16								
Heat Capacity (joule/kg-Kelvin)		963								
Thermal Contraction		Calculated								

Table C-5 Ontario climate stations detailed information (MTO 2016)

Station	Station Name	Location	Latitude	Longitude	Elevation (m)	Period (yyyymmdd)	
						From	To
15801	ARMSTRONG| ON	ARMSTRONG AIRPORT	50.294	-88.905	322	19530101	19680630
94932	ATIKOKAN| ON	ATIKOKAN	48.750	-91.617	395	19661001	19860930
15806	BIG TROUT LAKE| ON	BIG TROUT LAKE	53.833	-89.867	224	19700101	19891231
94862	CHAPLEAU| ON	CHAPLEAU	47.833	-83.433	428	19651101	19760331
94797	EARLTON| ON	EARLTON AIRPORT	47.700	-79.850	243	19591001	19790930
94864	GERALDTON| ON	GERALDTON	49.700	-86.950	331	19671101	19770331
94888	GERALDTON| ON	GERALDTON AIRPORT	49.783	-86.931	349	20000101	20070630
94803	GORE BAY| ON	GORE BAY AIRPORT	45.883	-82.567	194	19711001	19910930
14998	GRAHAM| ON	GRAHAM AIRPORT	49.267	-90.583	503	19530101	19661231
04797	HAMILTON| ON	HAMILTON AIRPORT	43.172	-79.934	238	20070101	20111231
14899	KAPUSKASING| ON	KAPUSKASING AIRPORT	49.414	-82.468	226	19870701	20121231
14999	KENORA| ON	KENORA AIRPORT	49.790	-94.365	410	19870701	20121231
94799	KILLALOE| ON	KILLALOE	45.567	-77.417	174	19530101	19720731
94805	LONDON| ON	LONDON AIRPORT	43.033	-81.151	278	19740201	19940131
94857	MOUNT FOREST| ON	MOUNT FOREST	43.983	-80.750	415	19620101	19760731
15804	NAKINA| ON	NAKINA AIRPORT	50.183	-86.700	325	19530101	19671031
04705	NORTH BAY| ON	NORTH BAY AIRPORT	46.364	-79.423	370	19740201	19940131
04772	OTTAWA| ON	MACDONALD-CARTIER INTERNATIONAL AIRPORT	45.323	-75.669	114	19870701	20111231
04706	OTTAWA| ON	OTTAWA ROCKCLIFFE AIRPORT	45.450	-75.633	54	19530101	19640331
54706	PETAWAWA| ON	PETAWAWA AIRPORT	45.950	-77.317	130	19730701	19930630
94842	SAULT STE MARIE| ON	SAULT STE MARIE AIRPORT	46.483	-84.509	192	19870701	20070630
94858	SIMCOE| ON	SIMCOE	42.850	-80.267	240	19620101	19770731
15909	SIOUX LOOKOUT| ON	SIOUX LOOKOUT AIRPORT	50.117	-91.900	383	19870701	20121231
04713	STIRLING| ON	STIRLING	44.317	-77.633	139	19530101	19681130
94828	SUDBURY| ON	SUDBURY AIRPORT	46.625	-80.799	347	19870701	20070630
94804	THUNDER BAY| ON	THUNDER BAY AIRPORT	48.369	-89.327	199	19740101	19931231
94831	TIMMINS| ON	VICTOR POWER AIRPORT	48.570	-81.377	295	19740701	19940630
54753	TORONTO| ON	BUTTONVILLE AIRPORT	43.862	-79.370	198	19870701	20121231
94791	TORONTO| ON	LESTER B. PEARSON INTERNATIONAL AIRPORT	43.677	-79.631	173	19870701	20070630
04715	TRENTON| ON	TRENTON AIRPORT	44.117	-77.533	86	19740601	19940531

Station	Station Name	Location	Latitude	Longitude	Elevation (m)	Period (yyyymmdd)	
						From	To
94808	WHITE RIVER| ON	WHITE RIVER	48.600	-85.283	379	19560101	19751231
94809	WIARTON| ON	WIARTON AIRPORT	44.746	-81.107	222	19750701	19950630
94810	WINDSOR| ON	WINDSOR AIRPORT	42.276	-82.956	190	19750701	19950630
15807	WINISK| ON	WINISK AIRPORT	55.233	-85.117	13	19590201	19650630

Table C-6. Percentage of trucks within design lane - recommended values for Ontario (MTO 2016)

Number of Lanes in One Direction	AADT (both directions)	Percentage of Trucks in Design Lane (%)
1	All	100
2	<15,000	90
	>15,000	80
3	<25,000	80
	25,000 to 40,000	70
	>40,000	60
4	<40,000	70
	>40,000	60
5	<50,000	60
	>50,000	60

Table C-7. Southern Ontario - typical axle per truck values (MTO 2016)

FHWA Class	Singles	Tandems	Tridems	Quads	Total
4	1.620	0.390	0.000	0.000	2.400
5	2.000	0.000	0.000	0.000	2.000
6	1.010	0.993	0.000	0.000	2.996
7	1.314	0.989	0.030	0.000	3.382
8	2.163	0.845	0.000	0.000	3.853
9	1.055	1.968	0.003	0.000	5.000
10	1.446	1.234	0.700	0.088	6.366
11	4.546	0.168	0.000	0.000	4.882
12	2.857	1.526	0.000	0.000	5.909
13	1.201	2.058	0.848	0.024	7.957

Table C-8 Northern Ontario - typical axle-per-truck values (MTO 2016)

FHWA Class	Singles	Tandems	Tridems	Quads	Total
4	1.620	0.390	0.000	0.000	2.400
5	2.000	0.000	0.000	0.000	2.000
6	1.014	0.993	0.000	0.000	3.000
7	1.244	0.962	0.043	0.000	3.297
8	2.414	0.674	0.000	0.000	3.762
9	1.048	1.955	0.014	0.000	5.000
10	1.358	1.165	0.840	0.044	6.384
11	3.849	0.538	0.000	0.000	4.925
12	2.910	1.514	0.021	0.000	6.001
13	1.100	2.012	0.945	0.011	8.003

Table C-9 Southern Ontario - single-axle load distribution (MTO 2016)

Axle Weight Range, kg	Frequency of a given axle weight range as a percentage									
	4	5	6	7	8	9	10	11	12	13
0 to 1249	1.80	0.07	0.19	0.28	0.42	0.04	0.39	0.10	0.02	0.44
1250 to 1749	0.96	0.33	0.14	0.08	0.42	0.10	0.17	0.09	1.10	0.63
1750 to 2249	2.91	5.40	0.89	0.45	2.13	0.62	0.44	0.57	0.02	0.85
2250 to 2749	3.99	7.52	0.73	0.70	2.43	0.43	0.89	1.69	3.22	1.21
2750 to 3249	6.80	6.65	0.95	0.87	3.55	0.44	0.93	6.75	8.16	1.14
3250 to 3749	12.00	11.32	2.12	0.96	7.82	0.62	1.44	5.58	8.73	1.02
3750 to 4249	11.70	13.98	4.73	1.51	7.20	1.22	1.48	4.29	8.70	0.99
4250 to 4749	11.40	13.94	13.96	3.14	19.16	10.40	4.39	11.03	14.49	4.93
4750 to 5249	10.30	10.71	18.40	5.10	13.03	22.56	12.86	14.92	15.75	12.59
5250 to 5749	9.00	10.46	24.84	8.07	11.20	40.89	28.90	11.09	15.01	33.61
5750 to 6249	7.40	5.04	10.66	3.70	3.96	14.54	15.17	7.09	6.42	17.86
6250 to 6749	5.70	4.36	8.60	9.64	6.09	3.05	6.91	10.44	5.54	8.99
6750 to 7249	4.30	2.28	4.54	11.08	5.70	1.04	3.37	7.90	4.18	3.33
7250 to 7749	3.20	1.95	3.67	13.64	3.76	0.92	3.46	6.14	2.13	2.35
7750 to 8249	2.58	1.65	1.45	11.34	2.12	0.90	3.14	3.66	1.42	1.29
8250 to 8749	1.80	1.25	1.54	6.99	3.03	0.83	3.46	2.95	1.03	1.58
8750 to 9249	1.40	0.80	1.37	5.97	1.45	0.49	2.87	1.75	0.32	1.08
9250 to 9749	1.00	0.73	0.42	3.87	1.57	0.28	3.12	0.87	0.83	2.32
9750 to 10249	0.75	0.50	0.36	5.90	1.41	0.16	1.96	0.66	0.00	0.72
10250 to 10749	0.50	0.51	0.23	2.27	0.95	0.13	1.55	0.38	0.10	0.98
10750 to 11249	0.25	0.27	0.04	1.73	0.59	0.11	1.15	0.14	0.08	0.49
11250 to 11749	0.15	0.08	0.04	0.23	0.26	0.06	0.38	0.43	0.11	0.21
11750 to 12249	0.10	0.06	0.02	0.25	0.18	0.03	0.35	0.19	0.19	0.18
12250 to 12749	0.00	0.07	0.04	0.47	0.31	0.03	0.23	0.00	0.71	0.08
12750 to 13249	0.00	0.02	0.00	0.04	0.12	0.01	0.11	0.75	1.27	0.17
13250 to 13749	0.00	0.01	0.00	0.18	0.11	0.01	0.10	0.00	0.00	0.06
13750 to 14249	0.00	0.01	0.00	0.11	0.06	0.01	0.13	0.18	0.24	0.18
14250 to 14749	0.00	0.01	0.00	0.00	0.32	0.00	0.10	0.07	0.00	0.00
14750 to 15249	0.00	0.01	0.05	0.06	0.11	0.01	0.05	0.18	0.00	0.09
15250 to 15749	0.00	0.01	0.00	0.22	0.12	0.01	0.13	0.00	0.00	0.24
15750 to 16249	0.00	0.00	0.00	0.13	0.05	0.01	0.10	0.04	0.00	0.10
16250 to 16749	0.00	0.00	0.00	0.02	0.14	0.01	0.04	0.03	0.00	0.00
16750 to 17249	0.00	0.00	0.00	0.23	0.13	0.01	0.07	0.00	0.00	0.10

17250 to 17749	0.00	0.00	0.00	0.09	0.08	0.02	0.04	0.04	0.00	0.00
17750 to 18249	0.00	0.00	0.00	0.00	0.00	0.00	0.01	0.00	0.00	0.12
18250 to 18749	0.00	0.00	0.00	0.37	0.02	0.00	0.03	0.00	0.00	0.01
18750 to 19249	0.00	0.00	0.02	0.06	0.00	0.00	0.01	0.00	0.00	0.04
19250 to 19749	0.01	0.00	0.00	0.16	0.00	0.01	0.04	0.00	0.23	0.00
19750 to 22749	0.00	0.00	0.00	0.09	0.00	0.00	0.03	0.00	0.00	0.02
Total	100	100	100	100	100	100	100	100	100	100

Table C-10 Southern Ontario - tandem-axle load distribution (MTO 2016)

Axle Weight Range, kg	Frequency of a given axle weight range as a percentage									
	4	5	6	7	8	9	10	11	12	13
0 to 2449	5.28	0.00	1.47	0.73	4.02	0.24	0.35	0.00	0.24	0.54
2500 to 3449	10.00	0.00	4.13	0.75	3.89	0.52	0.87	7.65	1.17	3.19
3500 to 4449	11.90	0.00	23.50	1.24	3.99	2.43	1.46	10.35	2.59	6.79
4500 to 5449	9.63	0.00	5.98	2.44	16.68	7.60	2.61	11.54	9.53	5.34
5500 to 6449	8.00	0.00	7.90	4.83	16.58	8.85	6.73	6.55	10.47	7.17
6500 to 7449	7.80	0.00	8.95	13.24	16.90	7.84	9.25	5.05	9.39	4.82
7500 to 8449	6.80	0.00	8.92	12.21	10.77	7.95	7.71	9.90	13.51	3.36
8500 to 9449	6.15	0.00	8.53	9.02	10.58	8.24	5.65	9.52	11.91	2.92
9500 to 10449	5.80	0.00	5.77	4.01	6.35	7.45	4.62	13.19	13.83	2.51
10500 to 11449	5.30	0.00	5.74	7.10	3.29	6.63	3.67	8.52	6.91	2.11
11500 to 12449	4.70	0.00	4.03	6.90	1.63	5.87	3.41	0.00	4.29	2.30
12500 to 13449	4.10	0.00	2.99	3.49	1.48	5.60	3.99	4.20	6.09	3.06
13500 to 14449	3.33	0.00	2.95	2.48	1.17	5.79	5.04	4.57	2.19	2.97
14500 to 15449	3.91	0.00	1.76	2.11	0.60	7.31	5.70	1.76	1.72	4.46
15500 to 16449	2.22	0.00	1.65	3.53	0.66	8.91	7.03	1.58	1.33	6.63
16500 to 17449	1.84	0.00	1.98	1.82	0.89	5.61	8.50	3.49	1.02	10.12
17500 to 18449	1.44	0.00	0.54	2.12	0.35	1.71	7.60	0.00	0.38	10.96
18500 to 19449	0.90	0.00	0.77	5.29	0.10	0.77	6.04	0.00	1.33	9.82
19500 to 20449	0.50	0.00	0.51	4.89	0.00	0.31	4.56	1.44	1.63	5.24
20500 to 21449	0.30	0.00	0.52	3.64	0.07	0.15	2.11	0.00	0.43	1.87
21500 to 22449	0.10	0.00	0.52	3.53	0.00	0.09	1.12	0.69	0.00	1.35
22500 to 23449	0.00	0.00	0.42	1.47	0.00	0.05	0.73	0.00	0.00	0.61
23500 to 24449	0.00	0.00	0.27	1.44	0.00	0.04	0.30	0.00	0.00	0.43
24500 to 25449	0.00	0.00	0.09	0.34	0.00	0.01	0.21	0.00	0.00	0.41
25500 to 26449	0.00	0.00	0.01	0.12	0.00	0.01	0.11	0.00	0.00	0.43
26500 to 27449	0.00	0.00	0.00	0.37	0.00	0.01	0.20	0.00	0.00	0.29
27500 to 28449	0.00	0.00	0.03	0.27	0.00	0.01	0.14	0.00	0.00	0.04
28500 to 29449	0.00	0.00	0.00	0.08	0.00	0.00	0.09	0.00	0.04	0.02
29500 to 30449	0.00	0.00	0.00	0.31	0.00	0.00	0.03	0.00	0.00	0.05
30500 to 31449	0.00	0.00	0.03	0.00	0.00	0.00	0.09	0.00	0.00	0.00
31500 to 32449	0.00	0.00	0.00	0.16	0.00	0.00	0.01	0.00	0.00	0.00
32500 to 33449	0.00	0.00	0.04	0.00	0.00	0.00	0.01	0.00	0.00	0.01
33500 to 34449	0.00	0.00	0.00	0.00	0.00	0.00	0.02	0.00	0.00	0.01

34500 to 35449	0.00	0.00	0.00	0.00	0.00	0.00	0.02	0.00	0.00	0.00
35500 to 36449	0.00	0.00	0.00	0.00	0.00	0.00	0.01	0.00	0.00	0.03
36500 to 37449	0.00	0.00	0.00	0.00	0.00	0.00	0.00	0.00	0.00	0.00
37500 to 38449	0.00	0.00	0.00	0.03	0.00	0.00	0.00	0.00	0.00	0.01
38500 to 39449	0.00	0.00	0.00	0.00	0.00	0.00	0.00	0.00	0.00	0.03
39500 to 40449	0.00	0.00	0.00	0.04	0.00	0.00	0.01	0.00	0.00	0.10
Total	100	100	100	100	100	100	100	100	100	100

Table C-11 Southern Ontario - tridem-axle load distribution (MTO 2016)

Axle Weight Range, kg	Frequency of a given axle weight range as a percentage									
	4	**5**	**6**	**7**	**8**	**9**	**10**	**11**	**12**	**13**
0 to 5249	0.00	0.00	0.00	4.26	0.00	39.94	4.98	0.00	0.00	6.50
5250 to 6749	0.00	0.00	0.00	9.29	0.00	7.55	9.65	0.00	0.00	11.02
6750 to 8249	0.00	0.00	0.00	10.96	0.00	19.96	9.53	0.00	0.00	6.55
8250 to 9749	0.00	0.00	0.00	0.30	0.00	5.90	7.21	0.00	0.00	3.69
9750 to 11249	0.00	0.00	0.00	14.23	0.00	0.67	5.21	0.00	0.00	2.44
11250 to 12749	0.00	0.00	0.00	1.97	0.00	5.34	5.07	0.00	0.00	2.29
12750 to 14249	0.00	0.00	0.00	4.54	0.00	2.18	4.39	0.00	0.00	2.18
14250 to 15749	0.00	0.00	0.00	2.12	0.00	8.20	4.32	0.00	0.00	4.16
15750 to 17249	0.00	0.00	0.00	12.24	0.00	3.58	4.56	0.00	0.00	4.46
17250 to 18749	0.00	0.00	0.00	0.64	0.00	1.74	4.82	0.00	0.00	4.54
18750 to 20249	0.00	0.00	0.00	0.00	0.00	3.42	5.87	0.00	0.00	3.90
20250 to 21749	0.00	0.00	0.00	0.50	0.00	1.23	5.44	0.00	0.00	7.33
21750 to 23249	0.00	0.00	0.00	0.00	0.00	0.00	6.96	0.00	0.00	11.94
23250 to 24749	0.00	0.00	0.00	9.88	0.00	0.00	6.31	0.00	0.00	14.87
24750 to 26249	0.00	0.00	0.00	3.00	0.00	0.29	5.68	0.00	0.00	8.24
26250 to 27749	0.00	0.00	0.00	6.69	0.00	0.00	4.50	0.00	0.00	3.49
27750 to 29249	0.00	0.00	0.00	9.24	0.00	0.00	2.20	0.00	0.00	1.43
29250 to 30749	0.00	0.00	0.00	4.56	0.00	0.00	1.25	0.00	0.00	0.34
30750 to 32249	0.00	0.00	0.00	5.58	0.00	0.00	0.60	0.00	0.00	0.35
32250 to 33749	0.00	0.00	0.00	0.00	0.00	0.00	0.32	0.00	0.00	0.16
33750 to 35249	0.00	0.00	0.00	0.00	0.00	0.00	0.31	0.00	0.00	0.04
35250 to 36749	0.00	0.00	0.00	0.00	0.00	0.00	0.25	0.00	0.00	0.01
36750 to 38249	0.00	0.00	0.00	0.00	0.00	0.00	0.28	0.00	0.00	0.06
38250 to 39749	0.00	0.00	0.00	0.00	0.00	0.00	0.11	0.00	0.00	0.00
39750 to 41249	0.00	0.00	0.00	0.00	0.00	0.00	0.04	0.00	0.00	0.00
41250 to 42749	0.00	0.00	0.00	0.00	0.00	0.00	0.05	0.00	0.00	0.00
42750 to 44249	0.00	0.00	0.00	0.00	0.00	0.00	0.09	0.00	0.00	0.01
44250 to 45749	0.00	0.00	0.00	0.00	0.00	0.00	0.00	0.00	0.00	0.00
45750 to 47249	0.00	0.00	0.00	0.00	0.00	0.00	0.00	0.00	0.00	0.00
47250 to 48749	0.00	0.00	0.00	0.00	0.00	0.00	0.00	0.00	0.00	0.00
48750 to 52749	0.00	0.00	0.00	0.00	0.00	0.00	0.00	0.00	0.00	0.00
100	100	100	100	100	100	100	100	100	100	100

Table C-12 Southern Ontario - quad-axle load distribution (MTO 2016)

Axle Weight Range, kg	Frequency of a given axle weight range as a percentage									
	4	5	6	7	8	9	10	11	12	13
0 to 5249	0.00	0.00	0.00	0.00	0.00	0.00	1.25	0.00	0.00	4.32
5250 to 6749	0.00	0.00	0.00	0.00	0.00	0.00	4.16	0.00	0.00	8.96
6750 to 8249	0.00	0.00	0.00	0.00	0.00	0.00	6.17	0.00	0.00	13.83
8250 to 9749	0.00	0.00	0.00	0.00	0.00	0.00	6.06	0.00	0.00	5.35
9750 to 11249	0.00	0.00	0.00	0.00	0.00	0.00	4.70	0.00	0.00	0.75
11250 to 12749	0.00	0.00	0.00	0.00	0.00	0.00	5.89	0.00	0.00	0.00
12750 to 14249	0.00	0.00	0.00	0.00	0.00	0.00	3.56	0.00	0.00	2.19
14250 to 15749	0.00	0.00	0.00	0.00	0.00	0.00	2.04	0.00	0.00	2.96
15750 to 17249	0.00	0.00	0.00	0.00	0.00	0.00	2.87	0.00	0.00	13.84
17250 to 18749	0.00	0.00	0.00	0.00	0.00	0.00	2.37	0.00	0.00	0.82
18750 to 20249	0.00	0.00	0.00	0.00	0.00	0.00	3.58	0.00	0.00	3.16
20250 to 21749	0.00	0.00	0.00	0.00	0.00	0.00	3.03	0.00	0.00	8.64
21750 to 23249	0.00	0.00	0.00	0.00	0.00	0.00	5.41	0.00	0.00	2.03
23250 to 24749	0.00	0.00	0.00	0.00	0.00	0.00	6.94	0.00	0.00	5.77
24750 to 26249	0.00	0.00	0.00	0.00	0.00	0.00	8.55	0.00	0.00	11.63
26250 to 27749	0.00	0.00	0.00	0.00	0.00	0.00	6.94	0.00	0.00	7.89
27750 to 29249	0.00	0.00	0.00	0.00	0.00	0.00	4.36	0.00	0.00	0.24
29250 to 30749	0.00	0.00	0.00	0.00	0.00	0.00	3.84	0.00	0.00	0.38
30750 to 32249	0.00	0.00	0.00	0.00	0.00	0.00	3.72	0.00	0.00	0.00
32250 to 33749	0.00	0.00	0.00	0.00	0.00	0.00	3.79	0.00	0.00	0.00
33750 to 35249	0.00	0.00	0.00	0.00	0.00	0.00	3.12	0.00	0.00	3.09
35250 to 36749	0.00	0.00	0.00	0.00	0.00	0.00	3.61	0.00	0.00	4.15
36750 to 38249	0.00	0.00	0.00	0.00	0.00	0.00	1.50	0.00	0.00	0.00
38250 to 39749	0.00	0.00	0.00	0.00	0.00	0.00	0.79	0.00	0.00	0.00
39750 to 41249	0.00	0.00	0.00	0.00	0.00	0.00	0.35	0.00	0.00	0.00
41250 to 42749	0.00	0.00	0.00	0.00	0.00	0.00	1.02	0.00	0.00	0.00
42750 to 44249	0.00	0.00	0.00	0.00	0.00	0.00	0.16	0.00	0.00	0.00
44250 to 45749	0.00	0.00	0.00	0.00	0.00	0.00	0.06	0.00	0.00	0.00
45750 to 47249	0.00	0.00	0.00	0.00	0.00	0.00	0.16	0.00	0.00	0.00
47250 to 48749	0.00	0.00	0.00	0.00	0.00	0.00	0.00	0.00	0.00	0.00
48750 to 52749	0.00	0.00	0.00	0.00	0.00	0.00	0.00	0.00	0.00	0.00
Total	100	100	100	100	100	100	100	100	100	100

Table C-13 Northern Ontario - single-axle load distribution (MTO 2016)

Axle Weight Range, kg	Frequency of a given axle weight range as a percentage									
	4	5	6	7	8	9	10	11	12	13
0 to 1249	1.80	0.20	0.22	0.00	2.14	0.06	0.63	5.59	0.59	0.15
1250 to 1749	0.96	0.61	0.00	0.00	1.88	0.09	0.20	0.00	0.00	0.46
1750 to 2249	2.91	11.58	0.47	0.26	5.38	0.61	0.66	0.00	2.59	0.58
2250 to 2749	3.99	10.37	0.35	0.00	6.19	0.42	0.66	0.00	1.27	0.61
2750 to 3249	6.80	8.26	0.09	0.03	7.42	0.22	1.61	5.59	2.50	1.04
3250 to 3749	12.00	11.40	7.08	0.17	9.96	0.77	2.06	0.00	6.41	1.13
3750 to 4249	11.70	11.52	8.11	0.32	13.50	1.20	2.21	1.96	4.29	1.47
4250 to 4749	11.40	12.33	10.21	3.28	13.60	4.72	3.17	6.93	12.67	3.71
4750 to 5249	10.30	8.79	14.42	5.52	7.22	11.71	9.34	16.96	5.81	12.37
5250 to 5749	9.00	8.64	30.26	3.80	8.18	42.47	27.56	4.48	22.17	33.59
5750 to 6249	7.40	3.72	9.15	9.29	2.61	23.52	19.40	10.05	14.30	25.58
6250 to 6749	5.70	2.32	5.20	23.71	4.02	4.64	8.64	1.96	6.63	10.57
6750 to 7249	4.30	3.04	4.34	9.42	3.75	2.47	3.75	13.96	8.89	1.60
7250 to 7749	3.20	1.53	3.12	17.49	4.88	1.94	3.57	13.47	1.44	1.41
7750 to 8249	2.58	0.62	2.29	4.60	3.01	1.40	3.00	0.00	0.00	0.91
8250 to 8749	1.80	1.66	1.45	2.23	1.26	0.66	3.31	7.03	1.04	1.67
8750 to 9249	1.40	1.14	1.62	4.85	0.74	0.69	3.19	0.00	3.26	0.84
9250 to 9749	1.00	0.90	1.41	4.02	1.42	0.38	2.37	7.03	0.00	0.91
9750 to 10249	0.75	0.51	0.00	6.21	0.17	0.24	1.10	3.03	0.00	0.22
10250 to 10749	0.50	0.12	0.00	1.78	0.00	0.25	1.19	0.00	0.00	0.21
10750 to 11249	0.25	0.05	0.00	1.16	0.79	1.20	0.76	0.00	3.26	0.00
11250 to 11749	0.15	0.42	0.21	0.29	0.74	0.08	0.27	0.00	1.25	0.06
11750 to 12249	0.10	0.15	0.00	0.25	0.00	0.04	0.10	1.96	0.59	0.00
12250 to 12749	0.00	0.12	0.00	1.15	0.00	0.06	0.29	0.00	0.00	0.07
12750 to 13249	0.00	0.00	0.00	0.00	0.00	0.00	0.35	0.00	1.04	0.00
13250 to 13749	0.00	0.00	0.00	0.00	0.00	0.02	0.17	0.00	0.00	0.00
13750 to 14249	0.00	0.00	0.00	0.00	0.00	0.01	0.07	0.00	0.00	0.00
14250 to 14749	0.00	0.00	0.00	0.00	0.82	0.02	0.04	0.00	0.00	0.28
14750 to 15249	0.00	0.00	0.00	0.00	0.00	0.03	0.08	0.00	0.00	0.00
15250 to 15749	0.00	0.00	0.00	0.00	0.32	0.01	0.09	0.00	0.00	0.00
15750 to 16249	0.00	0.00	0.00	0.02	0.00	0.00	0.05	0.00	0.00	0.11
16250 to 16749	0.00	0.00	0.00	0.00	0.00	0.02	0.01	0.00	0.00	0.00
16750 to 17249	0.00	0.00	0.00	0.14	0.00	0.02	0.05	0.00	0.00	0.12

17250 to 17749	0.00	0.00	0.00	0.00	0.00	0.02	0.01	0.00	0.00	0.23
17750 to 18249	0.00	0.00	0.00	0.00	0.00	0.01	0.00	0.00	0.00	0.03
18250 to 18749	0.00	0.00	0.00	0.00	0.00	0.00	0.00	0.00	0.00	0.07
18750 to 19249	0.00	0.00	0.00	0.01	0.00	0.00	0.00	0.00	0.00	0.00
19250 to 19749	0.01	0.00	0.00	0.00	0.00	0.00	0.03	0.00	0.00	0.00
19750 to 22749	0.00	0.00	0.00	0.00	0.00	0.00	0.01	0.00	0.00	0.00
Total	100	100	100	100	100	100	100	100	100	100

Table C-14 Northern Ontario - tandem-axle load distribution (MTO 2016)

Axle Weight Range, kg	Frequency of a given axle weight range as a percentage									
	4	5	6	7	8	9	10	11	12	13
0 to 2449	5.28	0.00	0.00	0.08	5.81	0.10	0.51	0.00	0.00	0.92
2500 to 3449	10.00	0.00	2.55	2.82	3.76	0.29	1.20	0.00	1.13	4.36
3500 to 4449	11.90	0.00	24.63	0.32	12.00	1.26	1.78	0.00	0.00	6.47
4500 to 5449	9.63	0.00	9.79	0.81	16.34	3.61	2.37	39.95	3.70	4.46
5500 to 6449	8.00	0.00	3.94	24.47	27.43	4.77	3.98	60.05	6.17	7.05
6500 to 7449	7.80	0.00	8.59	10.08	12.08	5.48	7.60	0.00	7.23	5.43
7500 to 8449	6.80	0.00	10.85	6.24	0.81	4.86	6.11	0.00	10.13	1.86
8500 to 9449	6.15	0.00	10.84	19.07	6.21	6.40	6.43	0.00	17.36	1.75
9500 to 10449	5.80	0.00	3.29	2.01	4.91	6.58	3.44	0.00	19.40	1.45
10500 to 11449	5.30	0.00	2.27	0.78	1.98	8.89	4.85	0.00	6.54	1.70
11500 to 12449	4.70	0.00	0.67	1.69	1.98	8.71	3.85	0.00	3.84	1.33
12500 to 13449	4.10	0.00	5.02	1.16	0.64	8.43	3.85	0.00	5.44	2.28
13500 to 14449	3.33	0.00	2.54	0.84	0.00	6.32	5.20	0.00	5.34	3.17
14500 to 15449	3.91	0.00	1.36	1.19	0.00	8.48	5.62	0.00	0.00	4.45
15500 to 16449	2.22	0.00	0.83	0.66	5.54	10.65	6.54	0.00	6.26	10.30
16500 to 17449	1.84	0.00	3.29	3.59	0.00	7.85	9.18	0.00	0.00	11.82
17500 to 18449	1.44	0.00	2.65	5.49	0.51	3.73	7.84	0.00	6.26	14.14
18500 to 19449	0.90	0.00	1.23	1.82	0.00	1.71	6.42	0.00	0.00	9.13
19500 to 20449	0.50	0.00	1.65	3.33	0.00	0.61	5.47	0.00	0.00	3.66
20500 to 21449	0.30	0.00	1.86	3.68	0.00	0.34	2.61	0.00	0.00	1.32
21500 to 22449	0.10	0.00	0.70	2.58	0.00	0.23	1.34	0.00	0.00	0.67
22500 to 23449	0.00	0.00	0.32	0.26	0.00	0.23	1.65	0.00	0.00	0.37
23500 to 24449	0.00	0.00	0.77	2.59	0.00	0.23	0.37	0.00	0.00	0.32
24500 to 25449	0.00	0.00	0.36	1.19	0.00	0.08	0.41	0.00	0.00	0.13
25500 to 26449	0.00	0.00	0.00	0.05	0.00	0.11	0.21	0.00	0.00	0.33
26500 to 27449	0.00	0.00	0.00	2.53	0.00	0.01	0.59	0.00	0.00	0.07
27500 to 28449	0.00	0.00	0.00	0.27	0.00	0.02	0.33	0.00	0.00	0.85
28500 to 29449	0.00	0.00	0.00	0.19	0.00	0.01	0.00	0.00	1.20	0.05
29500 to 30449	0.00	0.00	0.00	0.00	0.00	0.01	0.10	0.00	0.00	0.09
30500 to 31449	0.00	0.00	0.00	0.00	0.00	0.00	0.04	0.00	0.00	0.06
31500 to 32449	0.00	0.00	0.00	0.21	0.00	0.00	0.06	0.00	0.00	0.00
32500 to 33449	0.00	0.00	0.00	0.00	0.00	0.00	0.00	0.00	0.00	0.00
33500 to 34449	0.00	0.00	0.00	0.00	0.00	0.00	0.00	0.00	0.00	0.01

34500 to 35449	0.00	0.00	0.00	0.00	0.00	0.00	0.00	0.00	0.00	0.00
35500 to 36449	0.00	0.00	0.00	0.00	0.00	0.00	0.00	0.00	0.00	0.00
36500 to 37449	0.00	0.00	0.00	0.00	0.00	0.00	0.00	0.00	0.00	0.00
37500 to 38449	0.00	0.00	0.00	0.00	0.00	0.00	0.00	0.00	0.00	0.00
38500 to 39449	0.00	0.00	0.00	0.00	0.00	0.00	0.00	0.00	0.00	0.00
39500 to 40449	0.00	0.00	0.00	0.00	0.00	0.00	0.05	0.00	0.00	0.00
Total	100	100	100	100	100	100	100	100	100	100

Table C-15 Northern Ontario - tridem-axle load distribution (MTO 2016)

Axle Weight Range, kg	Frequency of a given axle weight range as a percentage									
	4	5	6	7	8		9	10	11	12	13
0 to 5249	0.00	0.00	0.00	0.00	0.00	7.03	5.26	0.00		0.00	5.63
5250 to 6749	0.00	0.00	0.00	20.16	0.00	5.16	7.54	0.00		100	13.67
6750 to 8249	0.00	0.00	0.00	0.00	0.00	0.00	8.63	0.00		0.00	6.55
8250 to 9749	0.00	0.00	0.00	44.60	0.00	0.19	6.67	0.00		0.00	2.23
9750 to 11249	0.00	0.00	0.00	9.52	0.00	0.85	4.91	0.00		0.00	2.02
11250 to 12749	0.00	0.00	0.00	0.00	0.00	5.33	4.48	0.00		0.00	1.16
12750 to 14249	0.00	0.00	0.00	0.00	0.00	1.04	4.85	0.00		0.00	1.75
14250 to 15749	0.00	0.00	0.00	0.00	0.00	77.00	5.07	0.00		0.00	2.42
15750 to 17249	0.00	0.00	0.00	0.00	0.00	0.13	5.21	0.00		0.00	3.41
17250 to 18749	0.00	0.00	0.00	0.00	0.00	0.00	4.96	0.00		0.00	4.27
18750 to 20249	0.00	0.00	0.00	0.00	0.00	2.79	7.72	0.00		0.00	4.74
20250 to 21749	0.00	0.00	0.00	0.00	0.00	0.00	6.05	0.00		0.00	10.07
21750 to 23249	0.00	0.00	0.00	13.18	0.00	0.00	5.54	0.00		0.00	13.11
23250 to 24749	0.00	0.00	0.00	12.54	0.00	0.28	6.90	0.00		0.00	17.57
24750 to 26249	0.00	0.00	0.00	0.00	0.00	0.20	5.38	0.00		0.00	6.99
26250 to 27749	0.00	0.00	0.00	0.00	0.00	0.00	4.27	0.00		0.00	2.47
27750 to 29249	0.00	0.00	0.00	0.00	0.00	0.00	2.05	0.00		0.00	0.51
29250 to 30749	0.00	0.00	0.00	0.00	0.00	0.00	1.57	0.00		0.00	0.48
30750 to 32249	0.00	0.00	0.00	0.00	0.00	0.00	0.98	0.00		0.00	0.27
32250 to 33749	0.00	0.00	0.00	0.00	0.00	0.00	0.87	0.00		0.00	0.07
33750 to 35249	0.00	0.00	0.00	0.00	0.00	0.00	0.47	0.00		0.00	0.55
35250 to 36749	0.00	0.00	0.00	0.00	0.00	0.00	0.29	0.00		0.00	0.06
36750 to 38249	0.00	0.00	0.00	0.00	0.00	0.00	0.18	0.00		0.00	0.00
38250 to 39749	0.00	0.00	0.00	0.00	0.00	0.00	0.09	0.00		0.00	0.00
39750 to 41249	0.00	0.00	0.00	0.00	0.00	0.00	0.04	0.00		0.00	0.00
41250 to 42749	0.00	0.00	0.00	0.00	0.00	0.00	0.00	0.00		0.00	0.00
42750 to 44249	0.00	0.00	0.00	0.00	0.00	0.00	0.00	0.00		0.00	0.00
44250 to 45749	0.00	0.00	0.00	0.00	0.00	0.00	0.00	0.00		0.00	0.00
45750 to 47249	0.00	0.00	0.00	0.00	0.00	0.00	0.02	0.00		0.00	0.00
47250 to 48749	0.00	0.00	0.00	0.00	0.00	0.00	0.00	0.00		0.00	0.00
48750 to 52749	0.00	0.00	0.00	0.00	0.00	0.00	0.00	0.00		0.00	0.00
Total	100	100	100	100	100	100	100	100		100	100

Table C-16 Northern Ontario - quad-axle load distribution (MTO 2016)

Axle Weight Range, kg	Frequency of a given axle weight range as a percentage									
	4	5	6		7	8	9	10	11	12	13
0 to 5249	0.00	0.00	0.00	0.00	0.00	0.00		3.18	0.00	0.00	5.82
5250 to 6749	0.00	0.00	0.00	0.00	0.00	0.00		5.32	0.00	0.00	9.55
6750 to 8249	0.00	0.00	0.00	0.00	0.00	0.00		10.24	0.00	0.00	3.11
8250 to 9749	0.00	0.00	0.00	0.00	0.00	0.00		5.20	0.00	0.00	0.00
9750 to 11249	0.00	0.00	0.00	0.00	0.00	0.00		2.00	0.00	0.00	0.00
11250 to 12749	0.00	0.00	0.00	0.00	0.00	0.00		3.36	0.00	0.00	0.00
12750 to 14249	0.00	0.00	0.00	0.00	0.00	0.00		2.61	0.00	0.00	3.12
14250 to 15749	0.00	0.00	0.00	0.00	0.00	0.00		2.12	0.00	0.00	6.44
15750 to 17249	0.00	0.00	0.00	0.00	0.00	0.00		4.23	0.00	0.00	3.85
17250 to 18749	0.00	0.00	0.00	0.00	0.00	0.00		2.47	0.00	0.00	9.36
18750 to 20249	0.00	0.00	0.00	0.00	0.00	0.00		1.01	0.00	0.00	0.00
20250 to 21749	0.00	0.00	0.00	0.00	0.00	0.00		0.23	0.00	0.00	0.00
21750 to 23249	0.00	0.00	0.00	0.00	0.00	0.00		7.58	0.00	0.00	3.41
23250 to 24749	0.00	0.00	0.00	0.00	0.00	0.00		3.05	0.00	0.00	2.40
24750 to 26249	0.00	0.00	0.00	0.00	0.00	0.00		4.19	0.00	0.00	45.88
26250 to 27749	0.00	0.00	0.00	0.00	0.00	0.00		7.42	0.00	0.00	0.09
27750 to 29249	0.00	0.00	0.00	0.00	0.00	0.00		3.19	0.00	0.00	6.97
29250 to 30749	0.00	0.00	0.00	0.00	0.00	0.00		5.90	0.00	0.00	0.00
30750 to 32249	0.00	0.00	0.00	0.00	0.00	0.00		6.43	0.00	0.00	0.00
32250 to 33749	0.00	0.00	0.00	0.00	0.00	0.00		5.29	0.00	0.00	0.00
33750 to 35249	0.00	0.00	0.00	0.00	0.00	0.00		4.38	0.00	0.00	0.00
35250 to 36749	0.00	0.00	0.00	0.00	0.00	0.00		8.46	0.00	0.00	0.00
36750 to 38249	0.00	0.00	0.00	0.00	0.00	0.00		1.64	0.00	0.00	0.00
38250 to 39749	0.00	0.00	0.00	0.00	0.00	0.00		0.00	0.00	0.00	0.00
39750 to 41249	0.00	0.00	0.00	0.00	0.00	0.00		0.00	0.00	0.00	0.00
41250 to 42749	0.00	0.00	0.00	0.00	0.00	0.00		0.00	0.00	0.00	0.00
42750 to 44249	0.00	0.00	0.00	0.00	0.00	0.00		0.50	0.00	0.00	0.00
44250 to 45749	0.00	0.00	0.00	0.00	0.00	0.00		0.00	0.00	0.00	0.00
45750 to 47249	0.00	0.00	0.00	0.00	0.00	0.00		0.00	0.00	0.00	0.00
47250 to 48749	0.00	0.00	0.00	0.00	0.00	0.00		0.00	0.00	0.00	0.00
48750 to 52749	0.00	0.00	0.00	0.00	0.00	0.00		0.00	0.00	0.00	0.00
Total	100	100	100	100	100	100		100	100	100	100

REFERENCES

AASHTO (2016). Mechanistic-Empirical Pavement Design Guide: A Manual of Practice. First Official Edition. American Association of State Highway and Transportation Officials, Washington DC.

AASHTO (2010). Guide for the Local Calibration of the Mechanical-Empirical Pavement Design Guide, American Association of State Highway and Transportation Officials, Washington DC.

AASHTO (2016). AASHTOWare Pavement ME Design Released Notes, http://me-design.com/MEDesign/Documents.html

Agardh, S. (2005). "Rut Depth Prediction on Flexible Pavement- Calibration and Validation of Incremental Recursive Model." Doctoral Thesis, Lund Institute of Technology, Sweden.

Ahmed, S (2017). "Local calibration of cracking models of MEPDG for Ontario's flexible pavement." Master Thesis, Ryerson University, Canada.

Al-Omari, B. and M.I. Darter (1992). Relationships Between IRI and PSR. Report Number UILU-ENG-92-2013. Springfield, IL: Illinois Department of Transportation.

Anderson, D. I., and D. E. Peterson (1979). Pavement Rehabilitation Design Strategies. FHWA UT-79/6. Salt Lake City: Utah Department of Transportation, 1979.

Arizona Department of Transportation Research Center (2014) "Calibration and Implementation of the AASHTO Mechanistic-Empirical Pavement Design Guide in Arizona". USA.

Bayomy, F., EI-Badawy, S., and Awed, A., (2012). "Implementation of the MEPDG for Flexible Pavements in Idaho." Idaho Transportation Department Research Program, FHWA-ID-12-193.

Caliendo, C. (2012). "Local calibration and implementation of the mechanistic-empirical pavement design guide for flexible pavement design." Journal of Transportation Engineering, 138(3), 348-360.

Crawford, G. (2009). "National Trends in Pavement Design." Southeastern States Pavement Management Association, Pavement Management and Design, New Orleans, Louisiana.

Crovetti, J. A., and Hall, K. T. (2012). "Local Calibration of the Mechanistic Empirical Pavement Design Software for Wisconsin." SPR #0092-09-30, SPR # 0092-09-31

Wisconsin Department of Transportation Research & Library Unit, 4802 Sheboygan Ave. Madison, WI 53707.

Darter, M. I., Titus-Glover, L., and VonQuintus, H. L. (2009). "Implementation of the Mechanistic–Empirical Pavement Design Guide in Utah: Validation, Calibration, and Development of the UDOT MEPDG User's Guide.", Utah Department of Transportation, Report No. UT--09.11.

Donahue, J. (2008). "Local calibration of the MEPDG for HMA pavements in Missouri." Journal of the Association of Asphalt Paving Technologists, Volume: 77, Asphalt Paving Technology 2008, 975-984.

Dzotepe, G. A., and Ksaibati, K. (2011). "The Effects of Environmental Factors on the Implementation of the Mechanistic-Empirical Pavement Design Guide (MEPDG)." Department of Transportation, University Transportation Center Program, University of Wyoming.

Glover, L. T. and Mallela, J. (2009). Guidelines for Implementing NCHRP 1-37A M-E Design Procedures in Ohio: Volume 4 - MEPDG Models Validation & Recalibration.

Gautam, G. P. (2015). "Local Calibration of MEPDG Rutting Model for Ontario's Superpave Pavements" Master Thesis, Ryerson University, Canada.

Haas, R. and Tighe, S. (2007). "Mechanistic-Empirical Pavement Design: Evolution and Future Challenges" Annual Conference Transportation Association of Canada.

Gramling, W. L., Hunt, J. E., and Suzuki, G. S. (1991). "Rational Approach to Cross-Profile and Rut Depth Analysis." Transportation Research Record, (1311), 173-179.

Hoegh, K., Khazanovich, L., and Jensen, M. (2010). "Local Calibration of Mechanistic-Empirical Pavement Design Guide Rutting Model for Minnesota Road Research Project Test Sections." Transportation Research Record, (2180), pp. 130-141.

Jadoun, F. M. (2011). "Calibration of the Flexible Pavement Distress Prediction Models in the Mechanistic-Empirical Pavement Design Guide (MEPDG) for North Carolina." Doctor of Philosophy, North Carolina State University, North Carolina.

Jannat, G. E. (2014) "Development of regression equations for local calibration of rutting and IRI as predicted by the MEPDG models for flexible pavements using Ontario's long-term PMS data" International Journal of Pavement Engineering, Vol. 17, No. 2, 166–175

Jannat, G. E. (2012). “Database Development for Ontario's Local Calibration of Mechanistic–Empirical Pavement Design Guide (MEPDG) Distress Models” Master Thesis, Ryerson University, Canada.

Kim, S., Ceylan, H., Ma, D., and Gopalakrishnan, K. (2014). “Calibration of Pavement ME Design and Mechanistic-Empirical Pavement Design Guide Performance Prediction Models for Iowa Pavement Systems,” ASCE Journal of Transportation Engineering, Vol. 21, Issue 10.

Kim, Y. R., Jadoun, F. M., Hou, T., and Muthadi, N. (2001). " Local Calibration of the MEPDG for Flexible Pavement Design." Final Report submitted to the North Carolina Department of Transportation, Research Project No. HWY-2007-07

Mallela, J., Glover, L. T., Sadasivam, S., Bhattacharya, B., Darter, M. I., and VonQuintus (2013). "Implementation of the AASHTO Mechanistic-Empirical Pavement Design Guide for Cororado." Colorado Department of Transportation, Applied Research Associates, Inc., Report No. CDOT-2013-4.

Missouri Department of Transportation (2009) Implementing The AASHTO Mechanistic Empirical Pavement Design Guide in Missouri, Volume II: MEPDG Model Validation and Calibration.

NCHRP (2001). Guide for Mechanistic-Empirical Design of New and Rehabilitated Pavement Structures. APPENDIX OO, http://onlinepubs.trb.org/onlinepubs/archive/mepdg/guide.htm

NCHRP (2004). Guide for Mechanistic-Empirical design of new and rehabilitated pavement structures. Appendix GG-1: Calibration of Permanent Deformation Models for Flexible Pavements., http://onlinepubs.trb.org/onlinepubs/archive/mepdg/guide.htm

NCHRP (2004). Guide for Mechanistic-Empirical design of new and rehabilitated pavement structures. Appendix GG-1: Calibration of Permanent Deformation Models for Flexible Pavements., http://onlinepubs.trb.org/onlinepubs/archive/mepdg/guide.htm

Paterson, W. D. O. (1989). “A Transferable Causal Model for Predicting Roughness Progression in Flexible Pavements.” Transportation Research Record 1215. Washington, DC: Transportation Research Board.

Thyagarajan, S. T. (2009). “Improvements to Strain Computation and Reliability Analysis of Flexible Pavements In The Mechanistic-Empirical Pavement Design Guide” Doctoral Thesis, Washington state University,USA.

Transportation Research Board, American Association of State Highway and Transportation, National Research Council, Washington, D.C.

VonQuintus, H. L., Mallela, J., Bonaquist, R., Schwartz, C. W., and Carvalho, R. L. (2012). "aNCHRP REPORT 719 Calibration of Rutting Models for Structural and Mix Design."

VonQuintus, H. L., and Moulthrop, J. S. (2007). "Mechanistic–Empirical Pavement Design Guide Flexible Pavement Performance Prediction Models for Montana.", Montana Department of Transportation, Helena, Montana.

Williams, D. R. C., and Shaidur, R. (2013). "Mechanistic-Empirical Pavement Design Guide Calibration for Pavement Rehabilitation." SPR 718 Institute for Transportation Iowa State University, 2711 South Loop Drive, Suite 4700 Ames, IA 50010-8664.

Waseem, A. (2013). "Methodology Development and Local Calibration of MEPDG Permanent Deformation Models for Ontario's Flexible Pavements" Master Thesis, Ryerson University, Canada.

"Weather stations for MEPDG in Ontario", accessed January 16, 2017, https://www.google.com/maps/d/viewer?msa=0&mid=13iBJ4hBSeGc_gTw_KJsEtwHXPXk.